Journal of the Geological Society, London, Vol. **159**, 2002, pp. 577–594. Printed in Great Britain.

The nature and provenance of accreted oceanic terranes in western Ecuador: geochemical and tectonic constraints

ANDREW C. KERR[1], JOHN A. ASPDEN[2], JOHN TARNEY[3] & LUIS F. PILATASIG[4]

[1]*Department of Earth Sciences, Cardiff University, Main Building, PO Box 914, Cardiff CF10 3YE, UK (e-mail: kerra@cardiff.ac. uk)*

[2]*British Geological Survey, Keyworth, Nottingham NG12 5GG, UK*

[3]*Department of Geology, University of Leicester, University Road, Leicester LE1 7RH, UK*

[4]*Dirección Nacional de Geología, Casilla, 17-03-23, Quito, Ecuador*

Abstract: Western Ecuador consists of a complex tectonic mélange of oceanic terranes accreted to the continental margin from Late Cretaceous to Eocene time. New geochemical data from these accreted terranes (arising from a 5 year British Geological Survey mapping programme) indicate that they comprise rocks from a variety of oceanic tectonic settings: from thickened (and relatively unsubductable) oceanic plateau basalts, through island-arc tholeiites, with occasional more calc-alkaline lavas, to back-arc basin basalt sequences. This study has enabled us to construct a new geodynamic model for the Cretaceous–Tertiary evolution of the Northern Andes, and has placed important new constraints on the extent of oceanic plateau sequences in Colombia and around the Caribbean. The age and nature of sediments, combined with evidence for the age of peak metamorphism, suggests that a prolonged (15–20 Ma) accretionary event occurred in Late Cretaceous time and involved the collision of an oceanic plateau (represented by the Pallatanga Unit) with the continental margin. This accreted unit can be correlated with similar oceanic plateau sequences from the Western Cordillera of Colombia and those within and around the Caribbean region. The Naranjal and Macuchi island arcs and the associated La Portada back-arc basin developed along the accreted margin from Late Campanian to Eocene time, and these arcs accreted to the continental margin along with oceanic plateau material (represented by the Piñon Unit and Pedernales–Esmeraldas sequences) during Eocene time. The development of island arcs, which separate the two accretionary events, implies that the most westerly (coastal) oceanic plateau sequences, both in Ecuador (Piñon and Pedernales–Esmeraldas) and in Colombia (Gorgona and Serranía de Baudó), cannot belong to the Caribbean–Colombian Oceanic Plateau (CCOP). It therefore appears that at least two different oceanic plateaux are preserved within the accreted oceanic terranes of the Northern Andes. It is possible that the CCOP formed over the Galápagos hotspot, as previously proposed, but the more westerly Coastal plateau was derived from a more southerly hotspot source region, such as Sala y Gomez, in the SE Pacific.

Keywords: Ecuador, oceanic plateaux, basalts, island arcs, accretionary wedges.

The growth of continental crust by subduction–accretion processes involving oceanic island arcs, marginal basins and, in particular, oceanic plateaux has been recognized by many workers (e.g. Abbott & Mooney 1995; Stein & Goldstein 1996; Polat *et al*. 1998; Puchtel *et al*. 1998; Condie & Abbott 1999; Kerrich *et al*. 1999; White *et al*. 1999). One of the major regions of continental crust growth over the past 150 Ma has been the western margin of the Northern Andes of South America (McCourt *et al*. 1984). Although the geochemical nature of the accreted Cretaceous and Tertiary terranes of western Colombia has been characterized in some detail (Millward *et al*. 1984; Kerr *et al*. 1996; 1997), the relationship of these terranes to those that occur within the Ecuadorian segment of the Northern Andes remains equivocal.

Between 1995 and 2000, the British Geological Survey (BGS) in partnership with the Corporacion de Desarrollo e Investigacion Geologico–Minero–Metalurgica (CODIGEM) carried out systematic geological mapping and geochemical (baseline) surveys of the Ecuadorian Cordillera Occidental between 1°N and 4°S over an area of *c*. 36 000 km^2. On the basis of this work we present a comprehensive set of new, high-precision, whole-rock geochemical data for the Cretaceous and Tertiary oceanic igneous rocks of western Ecuador. These data when used in conjunction with field evidence collected by the BGS–CODIGEM teams allow us to explore the possible correlations between Colombian and Ecuadorian units, and thus construct a new geodynamic model for the Cretaceous–Tertiary evolution of this portion of the Northern Andes. Furthermore, this study has provided important new insights into the spatial extent of the Caribbean–Colombian Oceanic Plateau (CCOP), suggesting that it may be composed of two different plateaux, derived from two separate mantle plumes.

Regional geology of western Ecuador and previous work

Geographically, Ecuador can be divided into three main areas; a western coastal plain (the Costa); a central Andean region (the Sierra) and the Amazon Basin (the Oriente) in the east. The Oriente is an extensive sedimentary basin, overlying older cratonic basement. The Andean Sierra comprises two mountain chains that are separated by a central inter-Andean valley or depression (Litherland & Aspden 1992). To the east is the Cordillera Real, which comprises metamorphic rocks, intruded

by early and mid-Mesozoic granitoids (Aspden & Litherland 1992; Aspden *et al*. 1992a, 1992b; Litherland *et al*. 1994). To the west of the inter-Andean valley, the Cordillera Occidental predominantly consists of fault-bounded Cretaceous–Tertiary accreted oceanic terranes, comprising basaltic volcanic and volcaniclastic rocks, which are the main focus of this study. The western margin of the inter-Andean depression is marked by a major structural feature: the Calacali–Pallatanga Fault Zone (Fig. 1) (Aspden *et al*. 1987a; Eguez & Aspden 1993). The Cordillera Occidental is intruded by Mid-Eocene to Late Tertiary granites and is overlain by post Late Eocene continental arc volcanic rocks. The geology of the Costa is less well known but it probably comprises a series of one or more marginal basins and is thought to be underlain by the basic oceanic crust of the Piñon Unit.

The term Piñon Formation was first introduced by Tschopp (1948) to refer to the mafic volcanic sequences that are present in the Ecuadorian Coastal Ranges, particularly in the area to the north of Guayaquil. Subsequent mapping by the French Petroleum Institute (see Faucher & Savoyat (1973) for a synthesis) in the 1960s led to an extension of Tschopp's original definition to include similar rocks that occur within the Cordillera Occidental that had previously been referred to simply as 'rocas verdes y porfidicas' (Wolf 1892) or more formally as 'Formacion Diabasica–Porfiritica' (Sauer 1965). Goosens & Rose (1973) proposed that both the Formacion Piñon and Formacion Diabasica–Porfiritica be renamed the Basic Igneous Complex and suggested a correlation with similar rocks from Costa Rica, Panama and Western Colombia.

As a result of a preliminary mapping survey (carried out by BGS and the then Ecuadorian Geological Survey (DGGM)) that included much of the Cordillera Occidental, Henderson (1979) proposed that the basic volcanic rocks of the Cordillera and the Costa were of a different age and origin. The name Piñon was restricted to the oceanic rocks of the Costa, whereas the name Macuchi Formation was created to include all the 'oceanic' rocks

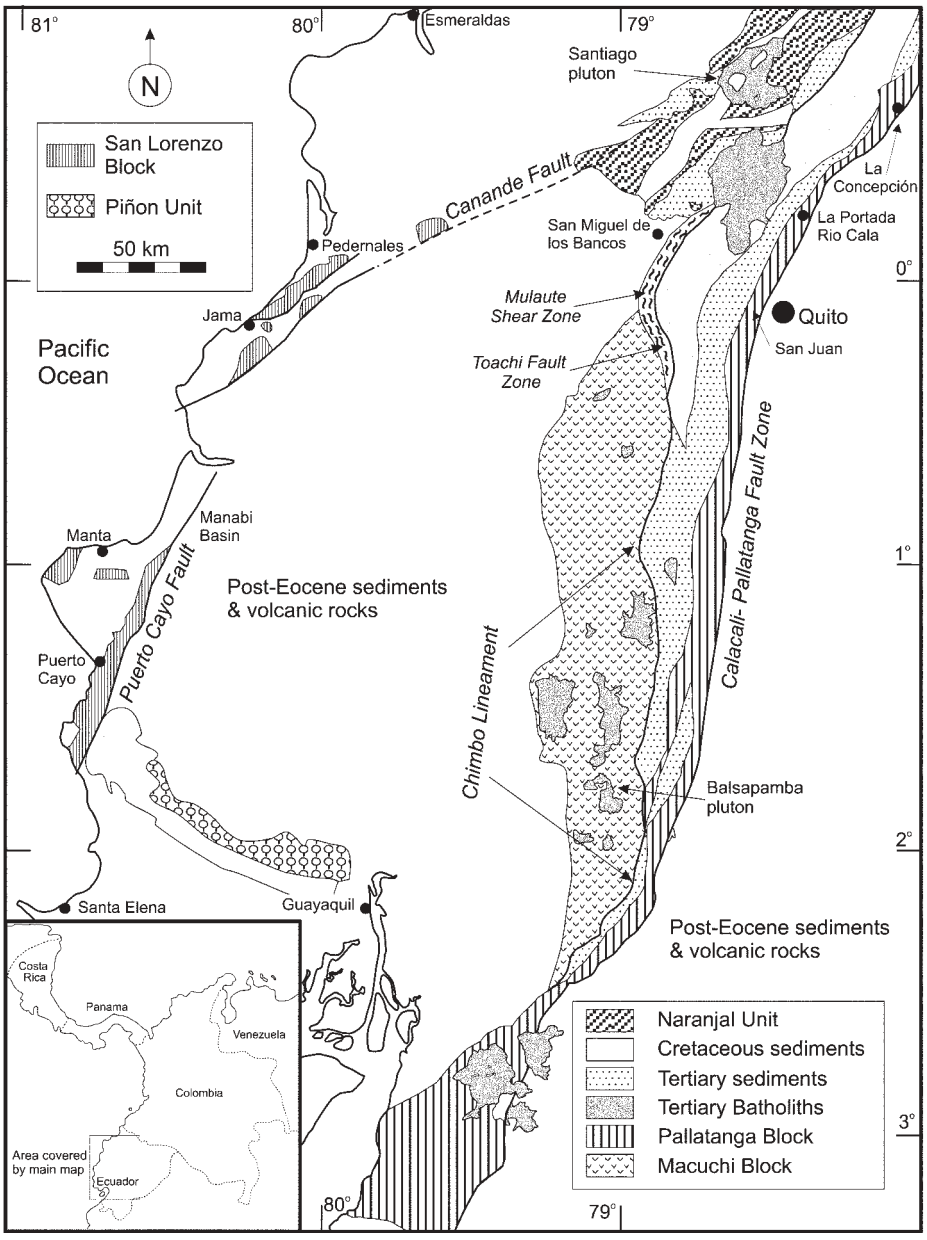

Fig. 1. Geological sketch map of Ecuador, showing the main units discussed in the text. The map is based on the five 1:200 000 maps published by CODIGEM–BGS for the Cordillera Occidental.

of the Cordillera Occidental, which were interpreted as island-arc volcanic rocks. On the basis of geochemical studies, Lebrat *et al*. (1985. 1987) suggested that the Macuchi Formation, as defined by Henderson (1979), included 'oceanic MORB [mid-ocean ridge basalt]' and calc-alkaline basalts in addition to island-arc tholeiites. The MORB rocks were correlated with the Piñon Formation of the Costa, and Van Thournout *et al*. (1992) also recognized similar volcanic sequences in the northwestern part of the Cordillera Occidental.

Within the past 5 years, detailed analytical geochemical studies have been carried out on the basalts of several localized areas of the Costa and the Cordillera Occidental south of Quito (Cosma *et al*. 1998; Reynaud *et al*. 1999; Lapierre *et al*. 2000); these studies have helped to shed new light on the origins of accreted Ecuadorian terranes.

Geology, petrology and age of the accreted igneous units

(Stratigraphic columns for the Cordillera Occidental and the Costa can be obtained from the Society Library or the British Library Document Supply Centre, Boston Spa, Wetherby, West Yorkshire LS23 7BQ, UK as Supplementary Publication No. SUP 18172 (5 pages).)

San Juan Unit

The oldest recognized igneous terrane within the Cordillera Occidental is the San Juan Unit (Eguez 1986), which is located some 10 km west of Quito (Fig. 1) and is up to 1 km wide by *c*. 10 km long. The Unit has previously been referred to by some workers as the Saloya Ultramafic Complex (e.g. Van Thournout 1991) and is in faulted contact with the Maastrichtian sediments of the Yunguilla Unit (Table 1) to the east and in probable faulted contact with the Pallatanga Unit to the west (Hughes & Bermudez 1997). The Unit comprises serpentinized peridotites, dolerites, anorthosite and hornblende-bearing gabbros (with possible ultramafic cumulate textures). Lapierre *et al*. (2000) have recently reported a three-point Sm–Nd isochron from one of the hornblende-bearing gabbros of the Unit, which has yielded an Aptian age of 123 ± 13 Ma.

Previous workers have variously interpreted the San Juan Unit as part of the arc-related Macuchi Unit (Henderson 1979) or as an ophiolite related to either a mid-ocean ridge (Eguez 1986; Lebrat *et al*. 1987; Van Thournout *et al*. 1992) or an oceanic plateau (Lapierre *et al*. 2000)

Pallatanga Unit

This Unit was defined by McCourt *et al*. (1997) and can be traced throughout much of the Cordillera Occidental, where it crops out as a series of discontinuous fault-bounded slices (Dunkley & Gaibor 1997; Pratt *et al*. 1997; Boland *et al*. 2000). Between 0 and 1°S these rocks are mainly overlain by younger volcanic deposits but, in regional terms, the eastern limit of the Pallatanga Unit coincides with the Calacali–Pallatanga Fault Zone, which, to the north of 2°S, also defines the eastern margin of the Cordillera Occidental (Fig. 1). To the south of 2°S the regional strike of both the Calacali–Pallatanga Fault Zone and the Pallatanga Unit are deflected as they progressively cut across the Cordillera before disappearing in the west below younger coastal alluvial deposits at 3°30′S.

Lithologically, the Pallatanga Unit typically consists of occasionally amygdaloidal and pillowed basalts, hyaloclastites and

Table 1. *Summary information on late Cretaceous–early Tertiary sedimentary units in western Ecuador*

Name	Latitude range	Structural position	Age	Lithology	Interpretation	Reference
Colorado Unit	0°15′N–1°00′N	Faulted against Naranjal	Camp	slst–congl	Marine turbidites, arc source	Boland *et al*. (2000)
Natividad Unit	0°04′S–0°45′N	Faulted against Pallatanga; Río Cala; La Portada	Camp–Maas	sst–mst–chert	Related to Río Cala arc	Boland *et al*. (2000)
Mulaute Unit	0°25′S–0°43′N	Faulted against Macuchi; Naranjal	Camp	slst–sst–brec	Marine turbidites, arc source	Hughes & Bermudez (1997)
Pilaton Unit	0°25′S–1°00′N	Faulted against Mulaute	Turon–Sen	cherts to brec	Marine turbidites, arc source	Eguez (1986)
Yunguilla Unit	3°18′S–0°37′N	Faulted against San Juan; Pallatanga; Natividad	Camp–Maast	mst–slst–sst	Related to Natividad	Boland *et al*. (2000)
R. Desgracia Unit	0°29′N–0°35′N	Faulted against Naranjal	Camp–Maas	mst–sst–congl	Marine turbidite; arc source	Boland *et al*. (2000)
La Cubera Unit	0°07′N–0°22′N	Faulted against Naranjal and Pallatanga	Paleo	chert–sst	Shallowing marine basin	Boland *et al*. (2000)
El Laurel Unit	0°44′N–0°55′N	Faulted against Pilaton	Eocene	shale–slst–sst	Lower part of marine fan	Van Thournout *et al*. (1992)
Silante Unit	0°37′S–0°43′N	Faulted against Macuchi and Pallatanga	Eocene–Oligo	slst–congl–brec–sst–lavas	Calc-alkaline arc source alluvial fan	Hughes & Bermudez (1997)
Tortugo Unit	0°14′S–0°43′N	Overlying La Cubera	Eocene	sst–slst	Deltaic–active volcanic source	Boland *et al*. (2000)
Angamarca Group	0°37′S–2°49′S	Faulted against Macuchi	Paleo–Eocene	sst–brec–slst–mst–	Shallowing marine basin	Boland *et al*. (2000)
Zapallo Unit	0°31′N–0°55′N	Unconformably overlying Naranjal and Río Desgracia	Eocene	congl–sst–mst	Arc source (Naranjal)	Boland *et al*. (2000)
Saruguro Unit	1°30′S–1°42′S	Unconformably overlying	Late	Lavas–tuffs	Calc-alkaline	Dunkley & Gaibor (1997)
	2°03′S–2°10′S	Pallatanga & interbedded	Eocene–		continental arc	
	2°45′S–3°45′S	with Angamarca Group	Miocene			

Camp, Campanian; Maas, Maastrichtian; Turon, Turonian; Sen, Senonian; Paleo, Palaeocene; Oligo, Oligocene; Mioce, Miocene; slst, siltstone; congl, conglomerate; sst, sandstone; brec, breccia; mst, mudstone

Table 2. *Representative chemical analyses of accreted oceanic rocks in western Ecuador*

Unit:	Pallatang	Pallatang	Pallatang	Pallatang	Pallatang	Pallatang	Pallatang	Pallatang	La Port	La Port	La Port
Latitude:	0–1°N	0–1°N	1–2°S	1–2°S	2–3°S	2–3°S	2–3°S	2–3°S	0–1°N	0–1°N	0–1°N
Sample:	M5-205	M5-211	M3-312	M3-313	PND905	PND1441	PND1482	PND1508	M5-300	M5-124	M5-125
SiO_2	48.46	50.67	51.20	50.65	51.04	50.79	48.95	49.38	46.34	47.83	48.23
TiO_2	1.78	1.04	1.43	1.44	0.91	1.54	1.94	0.98	0.23	0.33	0.30
Al_2O_3	12.52	14.03	14.20	15.11	14.40	14.23	14.02	13.34	11.54	16.23	14.49
Fe_2O_3*	14.79	12.43	12.66	12.25	11.47	13.74	15.26	11.32	11.12	10.67	9.17
MnO	0.27	0.18	0.19	0.21	0.19	0.21	0.21	0.18	0.20	0.14	0.14
MgO	5.49	7.47	7.02	7.53	8.03	7.22	5.78	10.22	12.48	10.34	8.26
CaO	12.41	10.15	8.91	8.64	10.98	9.67	10.27	12.87	17.48	10.57	14.35
Na_2O	4.08	3.99	3.96	3.37	2.17	2.64	1.82	1.59	0.33	2.79	2.60
K_2O	0.14	0.32	0.06	0.10	0.19	0.23	0.22	0.07	0.11	1.11	2.53
P_2O_5	0.18	0.09	0.13	0.11	0.08	0.13	0.18	0.08	0.03	0.05	0.05
Total†	100.12	100.37	99.76	99.40	99.46	100.40	98.66	100.02	99.86	100.07	100.13
LOI%	7.01	1.75	4.13	3.40	3.26	1.81	1.63	0.54	6.73	6.50	8.64
Trace elements (ppm)											
Sc	44.6	49.7	49.3	52.0	48.1	49.1	49.0	53.1	36.9	43.9	42.7
V	412	338	368	406	311	368	481	284	227	222	185
Cr	31	198	100	120	197	55	116	490	1915	522	403
Ni	47	91	72	99	104	63	75	142	365	138	96
Rb	0.73	3.33	0.67	0.97	2.38	7.23	5.25	1.14	1.21	19.16	37.89
Sr	39	142	49	126	131	124	114	123	37	115	117
Y	41.8	23.0	25.8	26.6	21.7	28.5	43.6	20.4	8.5	12.3	10.4
Zr	104	62	77	80	55	90	123	57	17	22	22
Nb	7.49	3.99	4.78	5.04	3.27	5.21	8.17	3.00	0.51	0.33	0.63
Ba	19	113	50	85	46	31	27	23	7	34	91
La	6.56	3.25	3.80	3.90	2.83	4.47	6.68	2.78	0.69	1.66	1.55
Ce	16.89	8.21	10.10	10.62	7.38	12.37	17.47	7.76	1.86	4.30	3.90
Pr	2.55	1.25	1.57	1.64	1.15	1.95	2.71	1.25	0.30	0.63	0.57
Nd	12.19	6.62	7.72	8.15	5.50	9.42	12.74	6.25	1.52	2.92	2.64
Sm	3.84	2.22	2.46	2.61	1.83	3.12	4.05	2.06	0.54	0.86	0.70
Eu	1.38	0.87	1.00	1.08	0.76	1.12	1.42	0.81	0.20	0.33	0.27
Gd	5.24	2.86	3.38	3.51	2.62	4.11	5.39	2.81	0.74	1.20	1.01
Tb	1.00	0.54	0.65	0.68	0.52	0.73	1.04	0.52	0.15	0.24	0.20
Dy	6.62	3.91	4.26	4.46	3.44	4.81	6.88	3.50	1.14	1.76	1.48
Ho	1.46	0.84	0.89	0.96	0.77	0.99	1.46	0.71	0.29	0.41	0.33
Er	4.24	2.54	2.69	2.78	2.22	2.82	4.37	2.07	0.93	1.32	1.03
Tm	0.67	0.37	0.39	0.42	0.36	0.42	0.68	0.32	0.15	0.23	0.18
Yb	4.28	2.36	2.58	2.64	2.29	2.74	4.35	2.02	1.11	1.48	1.26
Lu	0.63	0.36	0.39	0.37	0.34	0.40	0.66	0.28	0.19	0.23	0.19
Th	0.45	0.23	0.28	0.29	0.21	0.19	0.49	0.15	0.09	0.15	0.13

*Total Fe reported as Fe_2O_3.
†Totals reported on a dry basis.

massive dolerites. Whereas most of the dolerites and basalts are aphanitic, clinopyroxene- and plagioclase-phyric varieties are sometimes found (Dunkley & Gaibor 1997; McCourt *et al*. 1997). The aphanitic rocks possess variolitic and sub-ophitic textures, and evidence of quenching, in the form of sheaf-like aggregates of long curved, hollow plagioclase crystals, is common. Picrites are present (some are cumulates and some represent liquid compositions) but it must be stressed that they are relatively uncommon, as are intercalated volcaniclastic sediments and hyaloclastites. Occasional small gabbroic bodies intrude the sequence but these are volumetrically minor.

The Pallatanga Unit has thus far proved too altered to date by Ar–Ar step heating methods and K–Ar dating is of limited use in constraining the age of these rocks. A sequence of red mudstones on the Otavalo to Selva Alegre road (0°16′N; 78°28′W) intercalated with pillow basalts has yielded Santonian–Campanian fossil ages. Although on the basis of field evidence and preliminary geochemistry these pillow basalts were included within the Pallatanga Unit, the geochemical data presented in this paper reveal that these samples do in fact possess a subduction-related signature. It is therefore unlikely that these pillow basalts belong to the Pallatanga Unit and they are now thought to form a separate unit here named the La Portada Unit. Additionally, geochemical analyses reveal that several other small outcrops west and NW of La Concepción (0°37′N, 78°07′W; Fig. 1), originally mapped as Pallatanga, also have compositions similar to the La Portada Unit (Table 2).

This different petrogenetic association is also supported by the somewhat more westerly geographical position of these rocks compared with the Pallatanga Unit, the outcrops of which elsewhere at these latitudes are restricted to the easternmost margin of the Cordillera. Hence there are no firm age constraints for the Pallatanga Unit; however, Lapierre *et al*. (2000) have suggested that the Pallatanga basalts are genetically related to the San Juan Unit and are thus Aptian in age. Although we do not rule out this possibility, the fact that the two units are in faulted contact means that the age of the San Juan Unit cannot be used to constrain the age of the Pallatanga Unit. As we will discuss below, based on regional evidence, the lower age limit of this unit is considered to be pre-Senonian (i.e. >85 Ma).

Río Cala Unit

The Río Cala Unit (Boland *et al*. 2000) has been identified only from the 0–1°N sector of the Cordillera Occidental, with the main outcrops occurring in a fault block (*c*. 2 km × 12 km)

La Port 0–1°N M5-552	La Port 0–1°N M5-303	Piñon 2°S C1a	Piñon 2°S C1b	Piñon 2°S C2b	Nar Arc 0–1°N M5-394	Nar Arc 0–1°N M5-448	Nar Arc 0–1°N M5-456d	Nar Arc 0–1°N M5-658	Nar Arc 0–1°N M5-680	Nar Arc 0–1°N M5-687	Nar Arc 0–1°N M5-689	Nar Arc 0–1°N M5-740a	Nar Arc 0–1°N M5-740c
49.47	53.76	50.58	50.91	51.14	52.54	59.86	62.50	52.79	47.22	65.30	53.04	68.99	52.62
0.58	0.66	1.53	1.50	1.21	0.91	0.48	0.83	0.73	0.69	0.58	0.87	0.68	0.70
13.51	15.74	13.26	13.32	13.76	15.96	17.64	14.92	17.92	18.37	15.37	15.83	12.91	15.85
11.38	12.88	14.69	14.18	12.73	12.83	7.33	8.11	10.91	12.43	6.33	11.85	6.02	12.29
0.15	0.18	0.21	0.22	0.20	0.35	0.15	0.14	0.20	0.20	0.19	0.20	0.15	0.22
4.78	2.96	6.96	6.92	7.55	4.48	2.55	1.78	4.07	7.34	2.94	4.83	1.07	3.44
15.61	6.76	8.98	8.63	10.42	8.36	6.45	4.45	8.30	10.08	4.47	6.24	2.06	8.75
2.13	4.18	3.71	3.51	3.07	3.23	3.62	6.22	4.32	2.93	2.49	6.04	6.57	4.57
1.86	2.51	0.13	0.18	0.18	1.01	1.24	0.68	0.54	0.53	2.07	0.28	1.90	1.42
0.23	0.16	0.11	0.11	0.07	0.16	0.20	0.38	0.31	0.13	0.18	0.16	0.32	0.36
99.69	99.80	100.15	99.48	100.34	99.81	99.52	100.02	100.10	99.92	99.92	99.35	100.66	100.22
10.60	7.22	2.09	2.39	1.73	0.60	1.02	0.68	1.26	2.75	3.21	0.31	0.81	3.29
33.4	39.2	40.1	46.3	48.2	40.9	13.3	26.0	28.2	36.7	12.6	37.0	15.2	31.0
173	227	326	371	326	382	75	229	225	340	85	340	67	366
548	753	215	278	154	0	0	8	26	14	0	23	0	71
78	102	75	85	78	19	5	4	16	30	5	23	0	16
38.58	49.61	1.75	2.62	1.99	25.32	16.50	12.10	8.41	5.87	29.00	2.41	17.42	29.61
173	75	90	129	84	262	450	333	347	404	446	94	231	345
31.7	24.1	24.5	29.3	20.0	22.0	18.5	32.2	25.4	14.4	27.4	22.1	30.5	16.9
64	59	62	70	40	68	44	69	80	40	110	75	114	53
3.31	3.30	3.99	5.91	3.52	1.16	0.73	1.58	1.87	0.71	1.92	1.39	1.86	0.57
63	131	44	99	28	178	195	102	135	176	467	35	508	54
4.03	3.12	3.28	4.08	2.48	6.56	5.62	11.04	10.86	5.15	10.51	6.36	13.96	6.16
9.48	7.73	8.74	10.46	6.52	15.04	13.71	23.89	22.89	10.83	22.60	14.66	31.94	14.96
1.67	1.26	1.41	1.70	1.15	2.29	2.03	3.50	3.47	1.73	3.37	2.24	4.53	2.20
7.68	6.17	7.23	8.83	5.61	10.48	9.31	15.39	15.23	8.64	14.87	10.25	20.22	10.54
2.25	2.01	2.40	2.86	1.90	3.19	2.80	4.49	4.34	2.31	4.13	3.18	5.38	2.98
0.77	0.71	0.92	1.10	0.77	1.08	1.07	1.41	1.27	0.84	1.28	1.04	1.62	1.02
3.20	2.72	3.27	3.85	2.57	3.40	2.83	4.62	4.17	2.39	4.34	3.28	5.18	2.94
0.63	0.51	0.60	0.74	0.47	0.58	0.49	0.77	0.70	0.40	0.73	0.55	0.87	0.48
4.40	3.70	4.49	5.31	3.47	3.81	3.12	4.89	4.20	2.36	4.50	3.58	5.04	2.81
1.02	0.82	0.99	1.15	0.78	0.78	0.70	1.04	0.85	0.47	0.93	0.78	1.04	0.57
3.10	2.40	3.12	3.36	2.46	2.21	2.02	3.18	2.62	1.46	2.91	2.31	3.20	1.70
0.51	0.36	0.48	0.51	0.38	0.35	0.31	0.49	0.40	0.21	0.45	0.34	0.49	0.25
3.34	2.45	3.13	3.27	2.39	2.18	2.02	3.16	2.55	1.36	2.92	2.20	3.25	1.67
0.51	0.37	0.48	0.55	0.39	0.34	0.30	0.47	0.41	0.22	0.46	0.34	0.51	0.26
0.31	0.28	0.27	0.35	0.20	0.80	0.36	1.00	1.08	0.48	1.15	0.83	1.16	0.41

several kilometres east of La Portada (Fig. 1). The Unit consists of massive basaltic andesite to andesite lavas and volcaniclastic rocks that characteristically carry prominent pyroxene phenocrysts. The age of the Unit is uncertain but it almost certainly postdates the Pallatanga Unit and is probably contemporaneous with the Campanian–Maastrichtian volcaniclastic turbiditic sediments of the Natividad Unit, which crop out immediately to the west (Boland *et al*. 2000).

Naranjal Unit

This recently defined Unit (Boland *et al*. 2000) occurs to the west of the Toachi Fault towards the western margin of the Cordillera Occidental between 0 and 1°N (Fig. 1) and comprises a sequence of pillow basalts, basaltic to andesitic massive lavas and intrusions. Some of the basalts contain augite and plagioclase phenocrysts, whereas others are aphanitic or contain microphenocrysts of plagioclase (<1 mm) set in a matrix of feldspar laths, opaque minerals and pyroxene grains. The lavas are intercalated with igneous breccias, containing clasts up to 50 cm in diameter, and purple–grey siliceous mudstones. At one locality on the Río Naranjal (0°15′N, 79°00′W), these sediments contain radiolarian fauna that give a Late Campanian–Maastrichtian age (Boland *et al*. 2000). The Naranjal Arc can probably be directly correlated with the Ricaurte Arc in southern Colombia (Spadea & Espinosa 1996), which consists of pillow basalts and andesites, together with more massive lavas and volcaniclastic and siliciclastic sediments of Campanian age (Spadea & Espinosa 1996).

Macuchi Unit

Following on from earlier definitions by Henderson (1979) and Eguez (1986), the Macuchi Unit has been redefined by McCourt *et al*. (1997) as an early Tertiary sedimentary and volcaniclastic submarine arc sequence with intercalated pillow lavas and minor intrusions of basaltic to basaltic andesite composition. The Unit is exposed on the western side of the Cordillera Occidental between 0° and 2°30′S, and is in faulted contact principally with the siliciclastic Paleocene to Eocene Angamarca Group to the east (Hughes & Bermudez 1997; McCourt *et al*. 1997). To the west, the Unit is buried below Quaternary deposits of the coastal plain and has an estimated minimum thickness of 2–2.5 km.

The main rock types, in approximate order of abundance, are: lithic-rich volcanic sandstones, breccias (with basaltic andesite fragments) and tuffs; volcanic siltstones; cherts; pillow breccias and hyaloclastites; dolerites and microporphyritic pillow basalts.

Table 2. *(continued)*

Unit:	Nar Arc	Nar Arc	Nar Arc	Nar Plat	Nar Plat	Nar Plat	Nar Plat	Nar Plat	Macuchi	Macuchi	Macuchi	Macuchi
Latitude:	0–1°N	0–1°N	0–1°N	0–1°N	0–1°N	0–1°N	0–1°N	0–1°N	0–1°S	0–1°S	0–1°S	0–1°S
Sample:	M5-773	M5-835	M5-1043	M5-870	M5-871	M5-873	M5-936	M5-1014	RH278	RH279	RH280	RH282
SiO_2	50.06	52.32	52.95	51.53	50.73	57.90	49.39	48.74	50.45	52.71	57.01	54.02
TiO_2	0.55	0.83	0.97	2.48	1.76	2.19	0.92	1.24	0.77	0.71	0.54	0.65
Al_2O_3	17.19	17.18	17.00	11.94	12.91	11.11	14.53	14.61	18.35	15.89	14.96	16.41
Fe_2O_3*	9.87	11.23	11.48	18.42	16.82	15.12	14.24	13.55	8.19	8.72	7.59	8.30
MnO	0.13	0.16	0.17	0.21	0.22	0.20	0.16	0.24	0.18	0.16	0.20	0.15
MgO	8.57	6.29	4.64	3.62	5.61	1.56	9.51	7.62	8.75	11.34	10.73	7.82
CaO	10.75	9.76	6.15	7.82	6.87	7.07	12.06	9.82	9.31	7.65	5.49	8.64
Na_2O	2.32	2.45	5.84	3.69	4.43	4.59	1.87	3.84	2.46	1.96	3.25	3.73
K_2O	0.17	0.16	0.82	0.29	0.11	0.04	0.17	0.23	1.37	0.52	0.04	0.15
P_2O_5	0.07	0.14	0.13	0.21	0.14	0.30	0.08	0.10	0.14	0.12	0.09	0.09
Total†	99.67	100.52	100.15	100.21	99.61	100.08	102.95	100.01	99.96	99.79	99.92	99.97
LOI%	3.32	1.10	2.17	1.57	1.68	1.17	2.43	1.85	3.38	2.98	4.14	2.77
Trace elements (ppm)												
Sc	66.5	40.6	35.6	47.9	50.3	34.4	47.0	49.4	35.6	34.9	33.2	30.4
V	314	333	393	595	465	26	283	343	230	217	214	229
Cr	42	15	16	1	28	18	417	166	213	374	374	235
Ni	46	17	23	33	57	1	135	93	132	243	176	149
Rb	2.48	0.75	11.38	4.20	1.31	0.42	3.85	1.65	39.64	0.69	0.37	1.93
Sr	265	293	272	142	87	59	131	118	306	142	53	106
Y	12.6	21.0	22.8	51.3	37.9	71.8	26.9	26.1	18.5	34.2	12.8	15.7
Zr	27	68	79	147	100	92	45	73	71	49	42	53
Nb	0.31	1.22	0.94	9.50	6.53	13.53	4.70	4.48	1.71	0.77	0.65	0.69
Ba	61	72	257	96	32	24	33	77	89	24	27	25
La	1.25	5.10	4.21	7.66	5.43	17.98	5.24	3.81	4.71	8.52	2.25	3.15
Ce	3.40	13.15	11.22	18.96	13.74	39.98	10.49	9.94	10.91	16.81	5.52	7.86
Pr	0.59	2.11	1.82	2.89	2.15	5.61	1.50	1.54	1.62	2.11	0.87	1.25
Nd	3.39	10.26	9.16	15.71	11.24	27.82	7.83	7.83	7.51	9.65	4.45	6.01
Sm	1.26	2.91	2.80	5.07	3.81	8.37	2.40	2.62	2.39	2.58	1.45	1.76
Eu	0.47	1.02	1.04	1.78	1.35	2.45	0.92	1.05	0.83	0.94	0.50	0.77
Gd	1.61	3.18	3.35	6.09	4.74	10.15	3.15	3.52	2.61	3.49	1.67	2.17
Tb	0.31	0.54	0.57	1.25	0.91	1.89	0.58	0.64	0.42	0.66	0.33	0.40
Dy	2.11	3.36	3.67	7.96	6.22	12.21	3.78	4.15	2.78	4.33	2.01	2.55
Ho	0.47	0.73	0.79	1.70	1.31	2.50	0.84	0.93	0.60	0.98	0.42	0.54
Er	1.41	2.16	2.41	5.48	3.99	7.44	2.64	2.72	1.80	2.98	1.28	1.50
Tm	0.22	0.33	0.38	0.80	0.63	1.07	0.38	0.43	0.29	0.47	0.19	0.25
Yb	1.43	2.17	2.38	5.39	4.11	6.89	2.30	2.90	1.99	2.97	1.39	1.62
Lu	0.21	0.34	0.37	0.91	0.66	1.08	0.39	0.44	0.30	0.44	0.23	0.23
Th	0.16	0.67	0.53	0.51	0.40	0.39	0.30	0.28	0.49	0.25	0.32	0.35

Petrographically, the volcanic rocks comprise microphenocrysts of plagioclase with varying amounts of clinopyroxene, amphibole and olivine microphenocrysts set in an altered groundmass of plagioclase, opaque minerals, amphibole, chlorite and some glass.

Much of the disagreement in the literature regarding the age of the Macuchi Unit stems from the original definition of the Macuchi Formation by Henderson (1979), which included not only the Pallatanga, San Juan and Macuchi Units (as used in this paper) but also a sequence of marine Upper Cretaceous turbidites (now referred to as the Pilaton Unit), from which a poorly preserved specimen of the late Cretaceous (Senonian) ammonite *Inoceramus peruanus* and a sparse foraminifera fauna (Faucher & Savoyat 1973) had been recovered. Accordingly, the Macuchi Formation, as thus defined, ranged from (late) Cretaceous to Eocene in age. More recent work in the Cordillera Occidental, especially that of Eguez (1986) but including the present investigation (Hughes & Bermudez 1997; McCourt *et al*. 1997), has led to a reassessment of Macuchi 'Formation'. Although the age of the Unit is still not well established, the currently available evidence suggests that it is at least, in part, of early to possibly mid-Eocene age. However, on the basis of regional correlations it is possible that Macuchi activity began during Paleocene time and thus it is contemporaneous with the Timbuqui Arc in SW Colombia. The Timbuqui Arc is located along the western flanks of the Cordillera (around 2°30′N), where it is separated from the Western Cordilleran plateau basalt sequences by a major shear zone (McCourt *et al*. 1990).

Piñon Unit

The Cretaceous igneous basement of the Costa in Ecuador has often been referred to as the Piñon Formation by earlier workers, but the use of the term has, in some cases, become rather confused in the literature. In keeping with the informal lithostratigraphic nomenclature used in the Cordillera Occidental, we would therefore prefer to use the term Piñon Unit, which is defined herein as a sequence of pillow basalts and associated hyaloclastites, together with associated massive dolerite sills and dykes and occasional gabbros and peridotites. The Unit occurs in two different, but juxtaposed, sequences. One sequence occurs west of Guayaquil and is separated from the other, the Manabi–Pedernales–Esmeraldas sequence, by the Puerto Cayo–Canande Fault Zone (Fig. 1).

To the east of the Puerto Cayo–Canande Fault Zone (west of Guayaquil) good outcrops of the Piñon Unit are possibly

Macuchi 0–1°S RH122	Macuchi 0–1°S RH258A	Macuchi 0–1°S RH274	Macuchi 0–1°S RH276	Macuchi 1–2°S M3 190	Macuchi 1–2°S M3 485	Macuchi 1–2°S M3 518	Macuchi 1–2°S M3 761	Rio Cala 0–1°N M5-297	Rio Cala 0–1°N M5-1	Rio Cala 0–1°N M5-158	Rio Cala 0–1°N M5-82	Rio Cala 0–1°N M5-299	San Lor 1–2°S C10a
62.99	58.68	56.40	51.51	54.93	50.63	53.80	54.52	54.82	50.24	53.52	51.67	57.22	54.62
0.48	0.61	0.69	0.70	0.49	0.66	0.91	1.18	0.61	0.64	0.74	0.78	0.47	0.96
11.79	16.39	16.30	16.38	16.05	19.63	19.17	17.42	14.66	15.83	17.10	16.74	18.70	15.32
7.59	7.15	9.98	8.74	9.51	10.63	10.00	12.07	8.77	9.66	9.23	10.30	7.87	12.41
0.20	0.17	0.18	0.21	0.22	0.14	0.19	0.31	0.13	0.13	0.15	0.15	0.15	0.21
3.73	4.70	3.96	7.42	6.30	9.74	3.39	4.52	9.19	8.30	6.42	5.78	4.17	4.08
8.38	6.49	8.28	10.51	9.83	5.44	9.30	5.61	9.52	11.10	6.67	8.01	4.04	8.35
4.34	3.56	2.88	3.99	1.69	1.84	2.50	3.65	2.10	2.36	3.36	3.95	5.03	2.81
0.05	1.68	0.70	0.08	0.60	0.87	0.76	0.35	0.20	1.34	2.41	2.43	2.15	1.67
0.10	0.18	0.10	0.13	0.10	0.07	0.18	0.20	0.12	0.20	0.44	0.38	0.16	0.31
99.66	99.63	99.48	99.66	99.71	99.66	100.19	99.82	100.11	99.81	100.04	100.20	99.98	100.75
1.73	2.63	4.47	4.91	1.19	6.15	3.02	2.30	7.84	2.28	2.73	3.18	2.05	0.81
32.2	27.3	35.0	32.7	41.0	35.4	29.8	37.6	23.4	38.1	31.5	35.0	28.6	32.5
268	238	279	234	259	266	236	325	167	262	269	296	194	370
19	49	27	286	84	33	19	18	639	318	89	81	99	248
11	19	21	200	24	27	9	12	192	105	28	32	33	18
0.63	24.61	29.62	1.14	7.47	12.47	16.55	7.08	10.17	46.68	52.70	56.69	38.22	18.23
87	144	374	144	551	241	331	290	477	467	585	399	266	413
11.3	16.5	19.0	16.9	11.3	15.6	22.4	28.8	12.7	17.6	17.9	20.1	13.8	25.2
33	53	53	54	64	43	71	63	61	53	106	89	47	94
0.47	0.84	0.44	0.97	0.62	0.74	1.73	1.19	2.01	2.78	3.72	3.31	1.13	1.30
11	289	477	32	182	345	159	88	197	225	543	495	1845	250
1.74	5.34	3.64	3.65	7.52	2.89	7.00	5.87	5.00	6.64	22.45	18.67	7.43	11.56
4.34	12.40	7.03	8.73	15.30	8.23	16.22	14.08	11.25	14.25	49.07	41.22	15.08	27.16
0.68	1.75	1.18	1.40	2.15	1.32	2.43	2.31	1.64	1.92	6.41	5.43	2.01	4.02
3.85	8.14	5.60	6.54	9.34	6.31	11.01	11.53	7.11	8.60	25.64	22.50	9.02	19.77
1.25	2.33	1.76	1.95	2.51	2.00	2.94	3.79	1.86	2.59	5.07	4.75	2.43	4.96
0.47	0.75	0.78	0.71	0.80	0.84	1.13	1.31	0.68	0.87	1.68	1.56	0.88	1.37
1.62	2.46	2.41	2.45	2.12	2.34	3.58	4.12	2.21	2.79	5.15	4.84	2.34	4.60
0.30	0.42	0.45	0.43	0.35	0.42	0.61	0.75	0.35	0.46	0.65	0.65	0.37	0.81
1.77	2.57	2.91	2.75	2.01	2.66	3.80	4.82	2.17	2.85	3.40	3.72	2.26	4.95
0.38	0.58	0.65	0.58	0.39	0.57	0.79	1.04	0.43	0.58	0.62	0.67	0.48	1.00
1.18	1.69	1.90	1.70	1.08	1.69	2.35	3.00	1.25	1.63	1.73	2.06	1.39	2.89
0.18	0.27	0.29	0.27	0.16	0.28	0.37	0.46	0.18	0.25	0.26	0.30	0.22	0.44
1.26	1.74	2.02	1.79	1.09	1.68	2.42	3.09	1.23	1.67	1.71	1.98	1.50	2.73
0.18	0.28	0.30	0.27	0.16	0.26	0.36	0.49	0.18	0.25	0.25	0.29	0.23	0.40
0.19	0.76	0.35	0.41	1.75	0.57	0.95	0.63	0.59	1.51	2.58	2.03	1.11	1.18

stratigraphically overlain by pillow basalts of the Las OrquÍdeas Unit (Las OrquÍdeas 'Member' of Reynaud *et al*. 1999) and the 20 m thick Calentura Unit, comprising limestones, black shales and volcaniclastic tuffs. Although the Piñon Unit in the Guayaquil area is too altered to be dated by Ar–Ar step heating, the overlying Calentura Unit contains Late Cenomanian–Turonian foraminifera, Turonian ammonites and early Coniacian nannofossils (Jaillard *et al*. 1995). The occurrence of black shales within this unit further confirms its age, as the Cenomanian–Turonian boundary is marked by the worldwide occurrence of black shales (see review by Kerr 1998). Thus, if the Las OrquÍdeas and Calentura Units do stratigraphically overlie the Piñon Unit, this means that the top of the Piñon Unit west of Guayaquil must be at least of pre-late Cenomanian age (i.e. >94 Ma).

West of the Puerto Cayo and Canande faults, in the Manabi and Pedernales areas (Fig. 1) the Piñon Unit is overlain by, and is in faulted contact with, pillow basalts and sediments of the San Lorenzo Unit (see below) and is intruded by dykes of a similar chemical composition to the San Lorenzo Unit. In the ManabÍ area these dykes have been dated at 72.7 ± 1.4 Ma by ^{40}Ar–^{39}Ar (Lebrat *et al*. 1987), thus placing a minimum Campanian age on the basalts of the Piñon Unit east of the Puerto Cayo–Canande Fault Zone.

Petrographically, the basalts of the Piñon Unit are aphyric (with occasional plagioclase phenocrysts) and consist of plagioclase laths and clinopyroxene crystals set in a groundmass of small infilled vesicles, devitrified glass and dendritic clinopyroxene. The dolerites possess an ophitic texture with euhedral plagioclase, anhedral clinopyroxene and oxide minerals

San Lorenzo Unit

As discussed above, to the west of the of the Puerto Cayo and Canande faults the San Lorenzo Unit overlies and is in places in thrust contact with the Piñon Unit. The Unit consists of pillow basalts and andesites, ash layers, volcaniclastic conglomerates, thin limestones and turbidite-deposited sediments. In the southern portion of the Unit (around ManabÍ) intercalated sediments contain Late Campanian–Maastrichtian microfauna (Jaillard *et al*. 1995), which corroborates the Ar–Ar age for a San Lorenzo dyke reported above. In the more northerly outcrops of the Unit, the intercalated sediments contain Maastrichtian and Paleocene fossils (Jaillard *et al*. 1995). Petrographically, the rocks resemble those from the Piñon Unit except that they possess orthopyroxene and perhaps quartz in the groundmass.

Las Orquídeas Unit

This Unit, which overlies the Piñon Unit west of Guayaquil, was identified by Reynaud *et al*. (1999) and consists of a 'thin layer of pillowed phyric basalts'; however, no estimation of its thickness has been reported. Petrographically, the basalts possess plagioclase, clinopyroxene and orthopyroxene phenocrysts, set in a glassy matrix comprising crystals of plagioclase, clinopyroxene and oxides.

Cretaceous to Eocene sedimentary units and structural blocks in western Ecuador

Most of the sedimentary units present in the Cordillera Occidental (Table 1) are in fault contact with the accreted igneous units discussed above. With the exception of the quartz-rich Angamarca Group, many of these sequences contain a substantial proportion of igneous-derived material and are undoubtedly important in constraining the geodynamic history of western Ecuador, and their salient features are summarized in Table 1.

The igneous and sedimentary units in the Cordillera Occidental can be grouped into several structural blocks: the igneous units of Pallatanga, La Portada and Río Cala along with the sedimentary Natividad and Yunguilla Units (Table 1) comprise the Pallatanga Block, bounded to the east by the Calacali–Pallatanga Fault Zone and to the west by the Toachi Fault and its southern buried extension, the Chimbo lineament (Fig. 1). The Naranjal Block, located to the west of the Toachi Fault, consists of the igneous Naranjal Unit and the sedimentary Río Desgracia and Colorado Units. The Mulaute and Pilaton Units are of possible Late Cretaceous age and are located between the easternmost outcrop of the Naranjal Block and the westernmost outcrop of the Pallatanga Unit (Fig. 1). The Macuchi Block comprises the volcanosedimentary Macuchi Unit and, as we will discuss in more detail below, may also include the older (Paleocene to mid-Eocene) portions of the sedimentary Angamarca Group.

Analytical techniques

After removal of all weathered surfaces, the samples were crushed and powdered in an agate mill. The major elements along with Ni and Cr were analysed by XRF at the University of Leicester (see Kerr *et al*. (1997a) for more information). The rest of the trace elements including the REE were analysed by inductively coupled plasma mass spectrometry (ICP-MS) (Perkin Elmer, Elan 5000) at the Department of Earth Sciences, Cardiff University. Rock powder samples (0.1 g) were digested in concentrated $HF–HNO_3$. After evaporation the residue was dissolved with concentrated HNO_3, evaporated again and dissolved in 6 cm^3 of 5M HNO_3. The sample solution was accurately made up to 50 cm^3 with deionized water and a 2 cm^3 aliquot was spiked with a 100 ppb solution of Re and Rh, as internal standards, and made up to 10 cm^3 volume. A selection of international standard reference materials were used to calibrate the machine and W-2 was used as a drift monitor during analysis.

Representative data are presented in Table 2. The remainder of the data can be obtained from the Society Library or the British Library Document Supply Centre, Boston Spa, Wetherby, West Yorkshire LS23 7BQ, UK as Supplementary Publication No. SUP 18172 (5 pages).

Geochemical results

The geochemical classification and age ranges of all these igneous units are summarized in Table 3.

Table 3. *Tectonic setting and age ranges of Cretaceous igneous units in Ecuador*

Unit	Tectonic setting	Age
San Juan	Oceanic plateau?	Aptian
Pallatanga	Oceanic plateau	Cenomanian–Santonian
Río Cala	Calc-alkaline arc	Campanian–Maastrichtian
La Portada	Back-arc basin	Santonian–Campanian
Naranjal	Island-arc tholeiite	Campanian–Maastrichtian
Macuchi	Island-arc tholeiite	Late Paleocene–mid-Eocene
Piñon	Oceanic plateau	Pre-Cenomanian–Turonian
San Lorenzo	Calc-alkaline arc	Late Campanian–Maastrichtian
Las Orquídeas	Calc-alkaline arc	Cenomanian–Turonian

Pallatanga Unit

As outlined above, the predominant rock type in the Pallatanga Unit is basaltic and this is reflected in the whole-rock geochemistry of the rocks, with the majority of samples ranging from 7 to 9 wt% MgO (Figs. 2 and 3). On these diagrams, the Pallatanga samples have typical tholeiitic fractionation trends: higher TiO_2 and Fe_2O_3(t). In terms of their trace elements the Pallatanga basalts generally have higher concentrations of V, Sc, Y and Nb than the arc-related rocks (e.g. the Macuchi Unit) of the Cordillera Occidental. The Pallatanga samples possess low La/Yb ratios (<2.5) and high Zr/Th values (>200) (Fig. 4a). Primitive mantle-normalized multi-element plots and chondrite-normalized REE plots (hereafter multi-element plots and REE plots) show that the Pallatanga basalts possess essentially flat patterns (Fig. 5a and b).

Río Cala Unit

The samples collected from the Río Cala Unit possess a relatively wide range in MgO content from 4 to 8 wt% (Fig. 2). Al_2O_3 and SiO_2 (Fig. 2) broadly increase with decreasing MgO, whereas Fe_2O_3(t) decreases. The most evolved Río Cala sample possesses the lowest TiO_2. In terms of trace elements, the Río Cala lavas display no discernible trend for Sc, Nb, V and Y v. MgO (Fig. 3) whereas the REE and Zr generally increase with decreasing MgO. Sample M5-299 is an exception to this; although it is the most evolved Río Cala sample (lowest MgO, highest SiO_2), its incompatible trace element contents are anomalously low (Fig. 5c), in that it has similar trace element contents to M5-1, which is much less evolved. All the Río Cala samples show varying degrees of light REE (LREE) enrichment (La/Yb >4) and low Zr/Th ratios (<100) (Figs. 4a and 5c and d). These trace element ratios suggest that the lavas of the Río Cala Unit are of calc-alkaline affinity (Fig. 4a). A multi-element plot (Fig. 5c) reveals that all the Río Cala samples possess negative Nb and Ti anomalies.

La Portada Unit

The five analysed samples from this unit range in MgO content from 3 to 12.5 wt% MgO (Fig. 2). TiO_2, SiO_2, Y, Nb, Zr and the REE all broadly increase with decreasing MgO, whereas for other elements and oxides, there is no overall trend (Figs 2 and 3). The La Portada Unit possesses low La/Yb ratios (<1.3) and Zr/Th ratios ranging from 140 to 210 (Fig. 4a). The REE plot (Fig. 5d) shows that all of the samples have REE patterns that slope upwards from Gd to Lu, with $(Gd/Lu)_n < 0.7$, in contrast to all of the other groups of samples collected during the present

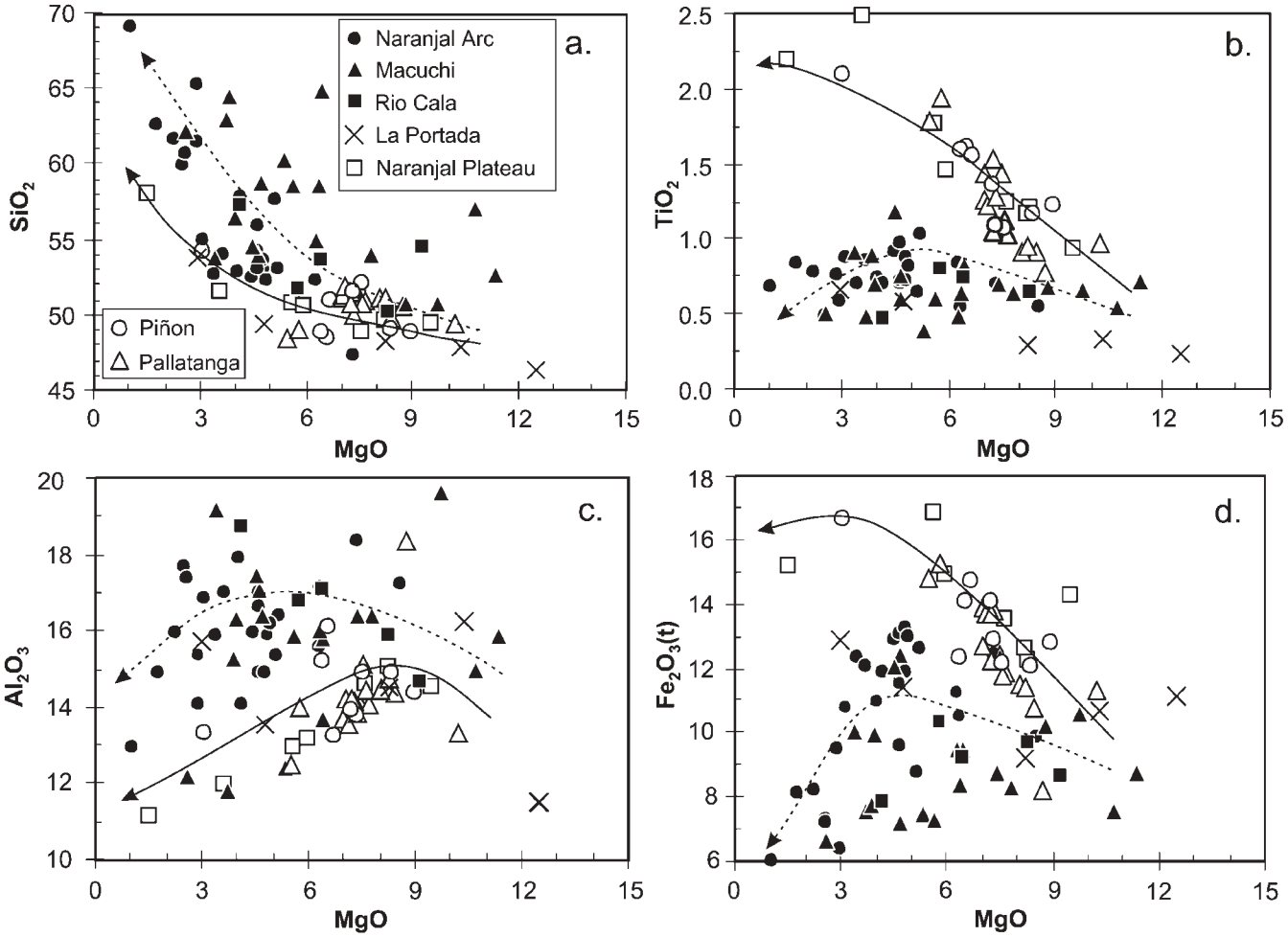

Fig. 2. Plots of major element oxides (wt%) v. MgO (wt%) for igneous units of the Costa and Cordillera Occidental of Ecuador. Arrows indicate approximate fractionation trends for the oceanic plateau sequences (continuous trend) and arc-related sequences (dashed trend).

study, which possess $(Gd/Lu)_n$ values of $\geqslant 1$. The La Portada samples are also variably enriched in the LREE (Fig. 5d) with the most primitive sample (M5-300) being depleted in the LREE, with $(La/Sm)_n = 0.8$, and the rest of the samples ranging from 1.0 to 1.5. A multi-element plot shows the La Portada samples displaying positive P anomalies and small relative depletions in Nb, Zr and Ti (Fig. 5c).

Naranjal Unit(s)

The igneous sequences of the Naranjal Unit are composed of two compositionally different types of rocks. As the two types cannot be readily differentiated in the field and do not occur in separate recognizable thrust blocks (although samples with chemical signatures similar to the Pallatanga basalts occur predominantly in the southwestern portion of the Naranjal structural block), they are for the time being regarded as subdivisions of the mapped Naranjal Unit. Whereas one group of the Naranjal basalts are chemically similar to the Pallatanga Unit and so are referred to here as 'Naranjal Plateau', the other group have chemical signatures similar to modern-day island-arc lavas (Fig. 5e and f) and are therefore referred to as the 'Naranjal Arc'.

The chemical difference between the two types can be observed in Figs. 2, 3 and 5e and f. The Naranjal Arc samples possess consistently lower TiO_2, $Fe_2O_3(t)$, Ni, V, Sc, Y, Nb and LREE than the Naranjal plateau samples at a given MgO content and they also contain higher SiO_2, Al_2O_3 and Th than the plateau rocks. These variations are also reflected in the trace element ratios (Fig. 4a), with the arc lavas showing La/Yb ratios that are generally >2, and Zr/Th ratios <180. In contrast, the plateau lavas have La/Yb <2.5 and Zr/Th >150. The differences between the two types are most clearly seen in Fig. 5c–f. It is clear from these diagrams that the arc lavas are enriched in Th and possess a characteristic negative Nb anomaly. The plateau lavas generally possess flat to slightly LREE-enriched chondrite-normalized patterns, whereas all but one of the arc lavas have negatively sloping REE patterns (Fig. 5d and f). One sample (M5-773), the most basic of the arc lavas (8.5 wt% MgO), is depleted in the LREE (Fig. 5d). It is interesting and perhaps significant that this sample comes from the easternmost edge of the Naranjal Unit.

Macuchi Unit

This unit is chemically similar to the Naranjal Arc, but the Macuchi lavas are generally more primitive (3–11 wt% MgO) than the Naranjal Arc samples (1–9 wt% MgO). At equivalent

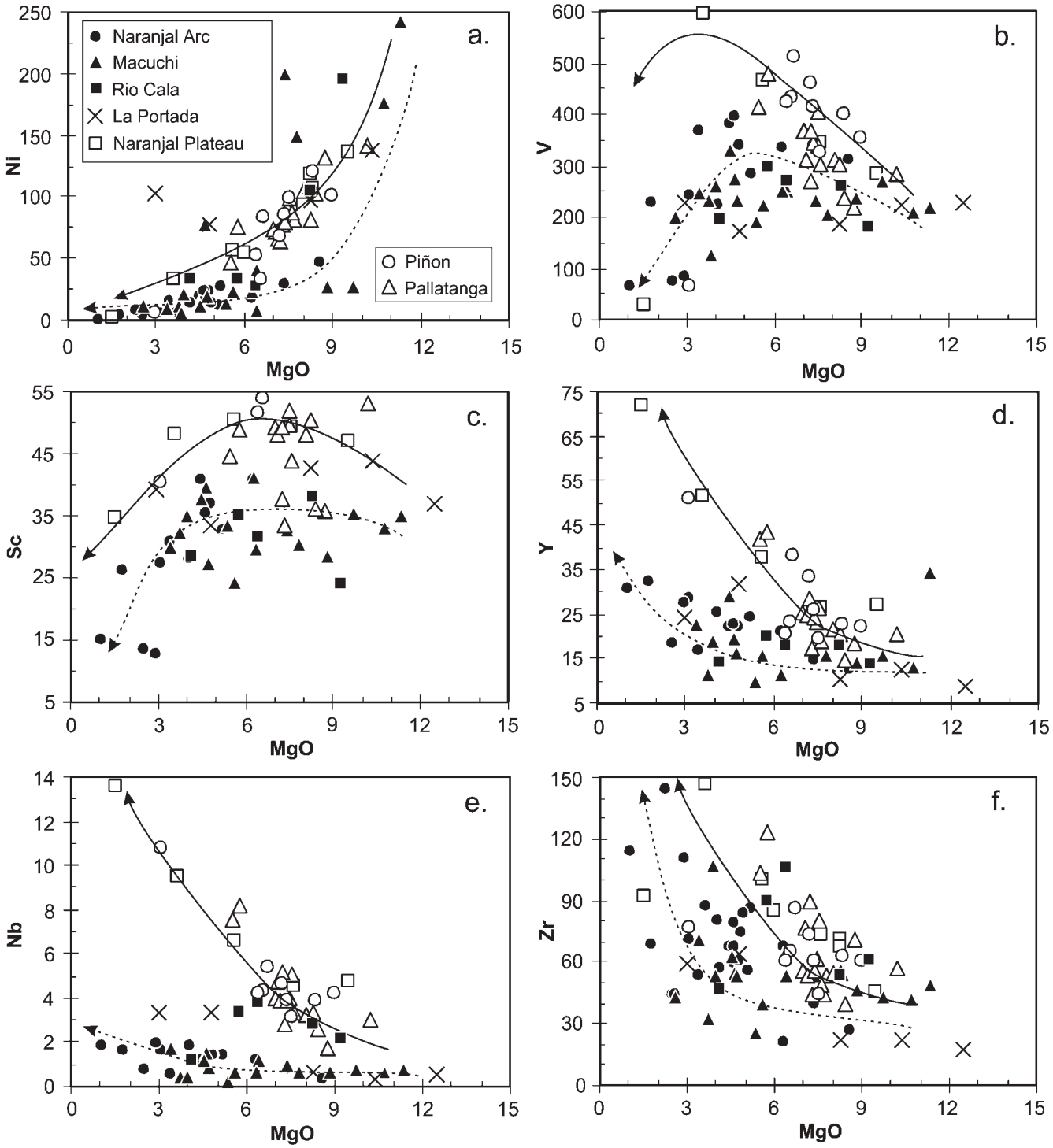

Fig. 3. Plots of trace elements (ppm) v. wt% MgO for igneous units of the Costa and Cordillera Occidental of Ecuador. Arrows indicate approximate fractionation trends for the oceanic plateau sequences (continuous trend) and arc-related sequences (dashed trend).

MgO contents the Macuchi lavas possess a similar range of major and trace elements to the Naranjal lavas (Figs. 2 and 3). Exceptions to this are SiO_2, which is significantly higher in the Macuchi Arc, and Fe_2O_3(t), V, Sc and Y, which are noticeably lower (Figs 2 and 3). The Macuchi lavas have Zr/Th values <200 and La/Yb ratios are for the most part below three (Fig. 4a). Multi-element plots display characteristic arc signatures such as negative Nb and Ti anomalies. Normalized REE patterns mostly display moderate LREE enrichment (Fig. 5g). Figure 5h reveals that several samples have different REE signatures from the majority of the Macuchi lavas: RH280 and RH122 possess REE contents that are more depleted, particularly in the LREE, whereas M3-190 has an REE pattern that is markedly enriched in the LREE (La/Yb >6) (Figs 4a and 5h).

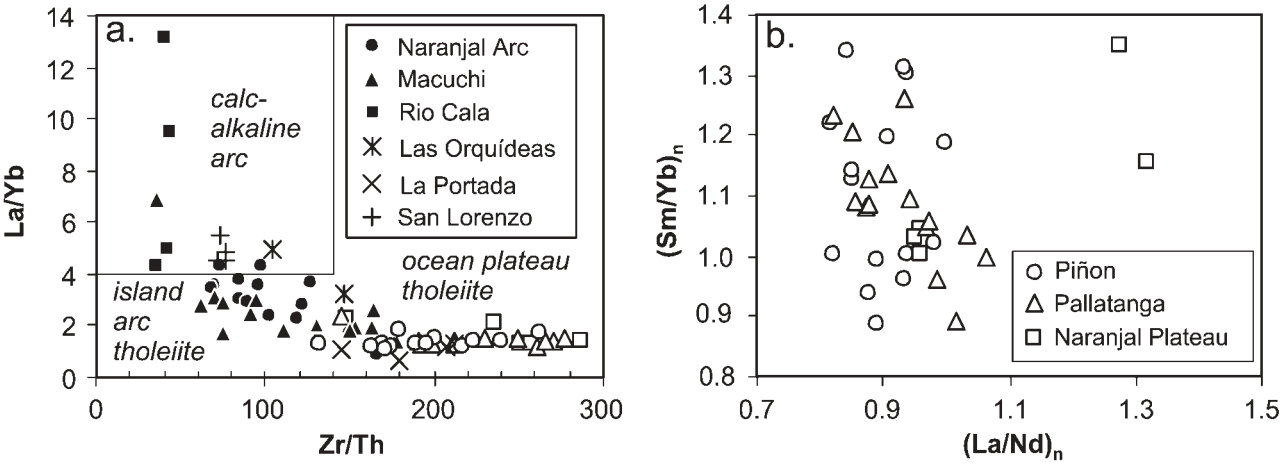

Fig. 4. (**a**) Plot of La/Yb v. Zr/Th showing all the igneous units of western Ecuador. Fields for calc-alkaline and tholeiitic compositions are adapted from Jolly *et al*. (2001). (**b**) Plot of $(Sm/Yb)_n$ v. $(La/Nd)_n$ showing Ecuadorian oceanic plateau rocks. Additional data for Las Orquídeas, San Lorenzo and Piñon are from Reynaud *et al*. (1999).

Piñon Unit

Three samples from the type area were collected during the present study (Table 2) and these supplement the published dataset of Reynaud *et al*. (1999). Both datasets are plotted in Figs 2 and 3 and all but one of the samples (a dolerite sill with 3.1 wt% MgO) possess MgO contents between 6 and 9 wt% MgO. The basalts and dolerites of the Piñon Unit are geochemically very similar to those of the Pallatanga Unit, with flat to slightly LREE-depleted REE patterns and near-identical multi-element patterns (Fig. 5a). The LREE patterns of the Piñon Unit are generally slightly more depleted than those of the Pallatanga Unit (Fig. 5b), a point also highlighted by the REE ratio–ratio plot (Fig. 4b), which reveals a trend towards lower $(La/Nd)_n$ ratios in the Pallatanga Unit.

San Lorenzo and Las Orquídeas Units

Lebrat *et al*. (1987) and Reynaud *et al*. (1999) presented several analyses from these Units, which have been plotted in Figs. 2, 3, 4a and 5g and h along with our sample from the San Lorenzo Unit. These lavas are all relatively evolved basaltic andesite compositions and are generally slightly more enriched in the most incompatible trace elements than either the Macuchi or Naranjal Arc samples. The San Lorenzo lavas possess La/Yb ratios >4 and Zr/Th ratios <150 (Fig. 4a) suggesting a calc-alkaline signature, similar to the Río Cala lavas of the Cordillera Occidental.

Only two analyses are available from the older (pre-Turonian) Las Orquídeas Unit (Reynaud *et al*. 1999); these samples are more basaltic than those of the San Lorenzo Unit, and possess lower abundances of incompatible elements. The lavas of the Las Orquídeas do, however, possess normalized patterns that are generally parallel to those of the San Lorenzo Unit (Fig. 5g and h).

Petrogenesis and tectonic setting

Pallatanga Unit (oceanic plateau)

The Pallatanga basalts, with their flat primitive mantle- and chondrite-normalized patterns, are very similar in chemical composition to basalts from the Caribbean–Colombian Oceanic Plateau (CCOP; Fig. 5a and b). The lack of a negative Nb anomaly eliminates the possibility of these rocks belonging to an arc-related sequence. Additionally, the Pallatanga Unit occupies a similar structural position to that of the accreted oceanic plateau sequences in the Western Cordillera of Colombia. On the basis of these considerations, the Pallatanga Unit probably represents accreted fragments of the CCOP. Picritic basalts and komatiites (as defined by Kerr & Arndt 2001) occur within the CCOP (Kerr *et al*. 1997b), but our extensive fieldwork throughout the Cordillera Occidental in Ecuador suggests that such rocks are rare within the Pallatanga Unit and volumetrically probably account for $<1\%$ of exposure.

Río Cala Unit (arc lavas)

The negative Ti and Nb anomalies of the Río Cala lavas are consistent with an arc-related origin for these rocks. Figures 2 and 3 reveal evidence for much earlier fractionation of clinopyroxene and titanomagnetite (lower Sc, V and Y), producing flatter trends on variation diagrams as compared with the Pallatanga basalts (Figs. 2 and 3). Of all the arc sequences preserved in the Cordillera Occidental, the Río Cala lavas are some of the most enriched in incompatible elements (including the REE) (Figs 4 and 5e–h). This enrichment could either represent a source characteristic or (more likely) could be explained by smaller degrees of melting below a thicker lithosphere. Thus, it is possible that the Río Cala lavas were formed below the thickened crust of 'Pallatanga oceanic plateau'. Sample M5-299 is the most evolved Río Cala sample, yet it possesses much lower abundances of incompatible trace elements than other slightly less evolved Río Cala samples (Fig. 3). Such low levels of incompatible trace elements may be produced by more extensive melting beneath thinner lithosphere, and hence suggest the possibility that a marginal basin may also have been associated with the development of the Río Cala Arc.

La Portada (back-arc basin)

The compositions of basalts and andesites of the La Portada Unit with their negative Ti and Nb anomalies (Fig. 5c) strongly suggest a subduction-related origin for this unit. These relatively

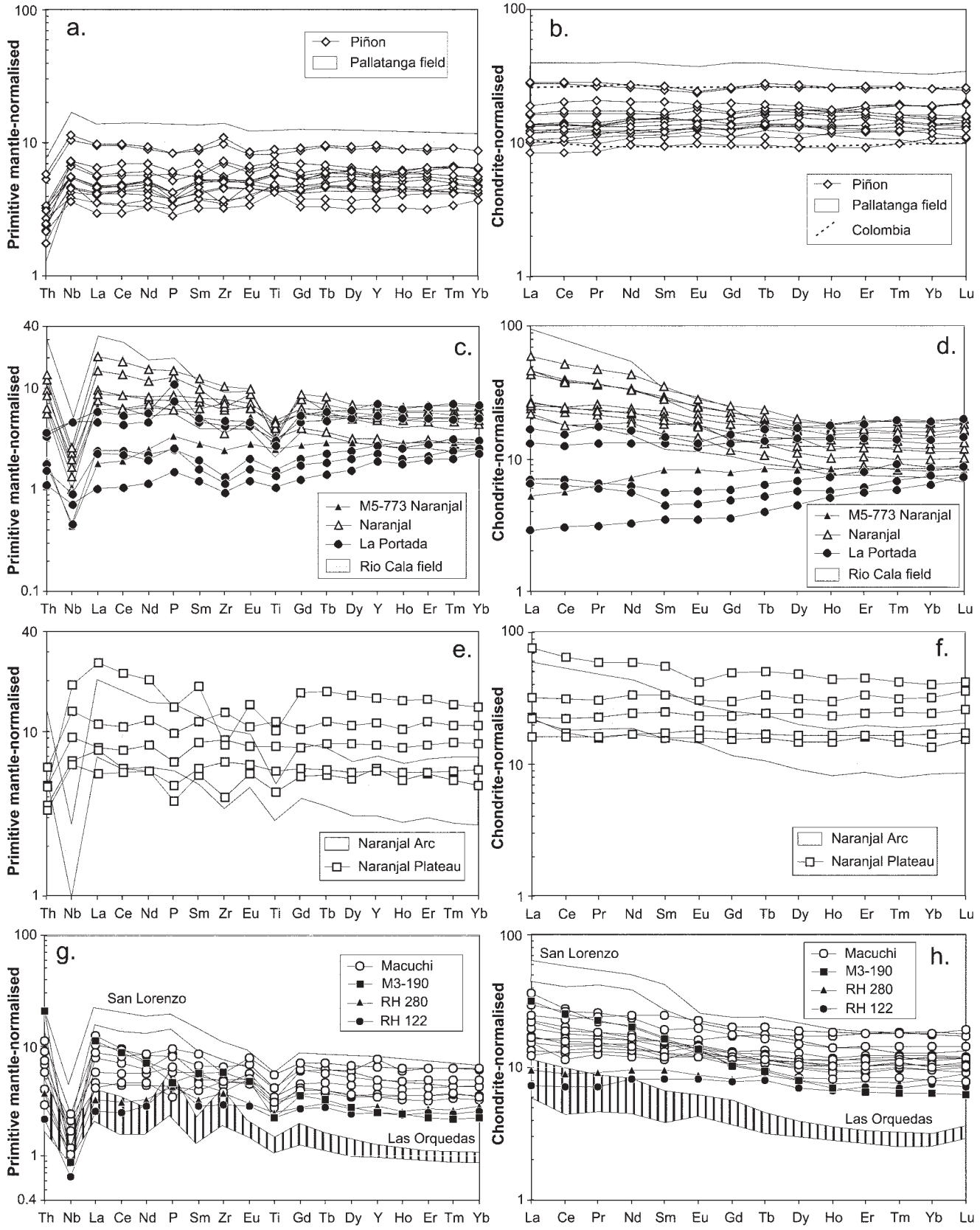

Fig. 5. Rare earth element and primitive mantle-normalized multi-element plots (normalizing values from Sun & McDonough 1989) showing all the igneous units in western Ecuador. Additional data for Las Orquídeas, San Lorenzo and Piñon are from Reynaud *et al*. (1999). In (**b**), the dashed boundary field for Colombia shows the compositional range of oceanic plateau lavas from the Western Cordillera of Colombia (Kerr *et al*. 1997a). Noteworthy samples from the Macuchi and Naranjal arc units are plotted separately in (**c**), (**d**), (**g**) and (**h**), and are discussed in the text.

primitive mafic lavas (Figs. 2 and 3) show only limited enrichment in incompatible elements [low $(Gd/Lu)_n$] (Fig. 5c and d), implying that there was a small source input from arc-derived fluids and sediments. Thus the source region of these rocks may have been some distance from an active arc, suggesting that the environment of formation may have been a marginal basin associated with either the Río Cala or the Naranjal Arcs.

Naranjal Unit(s) (island arc and oceanic plateau)

The arc-derived samples of the Naranjal Unit display compositions typical of modern-day island arcs, with moderate enrichments in the most incompatible elements (Fig. 5c). It is likely that sample M5-773, with its depleted LREE chondrite-normalized pattern (Fig. 5d), formed in a back-arc basin associated with the Naranjal Arc. A back-arc basin origin is further supported by the fact that the sample was collected from the easternmost margin of the Naranjal Unit. The geochemical similarity of this sample to the more depleted samples of the La Portada Unit is striking.

The plateau lavas that are associated with the Naranjal Unit have relatively flat REE patterns (Fig. 5f) and generally higher abundances of incompatible trace elements than those of the Pallatamga Unit. These characteristics, together with the fact that these rocks occur towards the westernmost margin of the Naranjal Unit outcrop, make it improbable that they belong to the same plateau as the Pallatanga and we propose that they represent the dismembered portions of a different oceanic plateau.

Macuchi Unit (island arc)

We have already noted the similarity in terms of their incompatible trace elements of the Macuchi Unit to the arc lavas of the Naranjal. However, the differences between the two arcs in terms of lower Fe_2O_3(t), V, Sc and Y (Figs. 2 and 3) may indicate the earlier onset of clinopyroxene and titanomagnetite fractionation in the Macuchi Arc than in the Naranjal. Trace element modelling using the TRACE program (Nielsen 1988) reveals that higher oxygen fugacity would result in the earlier fractionation of clinopyroxene in the Macuchi Arc than in the Naranjal. It is possible that the more primitive (higher MgO) and more depleted Macuchi lavas may have formed in a back-arc basin.

Piñon (oceanic plateau)

Given their similarity to other oceanic plateau lavas it is highly likely that the lavas and intrusions of the Piñon Unit also originated in an oceanic plateau. However, as we will discuss below, the Piñon Unit cannot belong to the same oceanic plateau as the Pallatanga Unit, as these two units are of the same age and accreted at different times. Furthermore, the Pallatanga and Piñon Units are separated by the Naranjal and Macuchi island arcs. A chemical difference between the two units is also evident in that the Piñon Unit has slightly more depleted LREE patterns (Fig. 4b), which would suggest either that it was derived from a more depleted source region or that it represents the product of a more extensive mantle melting event. It may be significant that a similar LREE depletion is also evident in the more westerly accreted oceanic plateau sequences that are preserved in the Serranía de Baudó (Kerr *et al*. 1997a) and Gorgona (Kerr *et al*. 1996) in Colombia.

San Lorenzo and Las Orquídeas Units (arc lavas)

The more incompatible element-enriched nature of the basaltic andesites of the San Lorenzo Unit (relative to Naranjal and Macuchi Arcs) is in part a reflection of their more evolved nature, but it is also due to the calc-alkaline affinity of the San Lorenzo lavas (i.e. $(La/Yb)_{cn} > 4$; $Zr/Th < 150$). Given that some of the San Lorenzo Arc lavas are seen to stratigraphically overlie an oceanic plateau sequence, their more enriched incompatible trace element signature may well be due to melting beneath the thickened oceanic crust at the trailing edge of the oceanic plateau.

The similarity in the shape of the chondrite-normalized patterns for lavas of the Las Orquídeas and the San Lorenzo Units is also noteworthy. The lavas of these units stratigraphically overlie the Piñon Unit and the steep chondrite-normalized patterns suggest that both arcs may well have formed by a low degree of partial melting beneath the thickened crust of an oceanic plateau.

Geological constraints on tectonic models

In addition to geochemical evidence for the original tectonic setting of the accreted igneous terranes in Ecuador a consideration of sedimentary, palaeontological, geochronological and structural constraints is vital in the elucidation of tectonic evolution models of the Northern Andes in Late Cretaceous–Early Tertiary time.

Pallatanga accretion

The timing of accretion of the Pallatanga Block is critical to tectonic evolution models of the region. Although there is little direct evidence for the age of accretion of the Pallatanga Block to the Andean continental margin, there are several pieces of information that do provide important constraints on the timing of this event. First, Aspden *et al*. (1992) noted a widespread resetting of isotopic ages in the Cordillera Real between 85 and 65 Ma. The absence of regional igneous activity at this time led to the interpretation that this resetting was most probably caused by the uplift of the Cordillera Real, which in turn was related to the arrival of the Pallatanga Block from the west and its subsequent accretion along the line of the Pallatanga Fault Zone. Second, and as a result of this uplift, continental Maastrichtian sediments were deposited along the eastern flank of the emergent Cordillera Real (Tena Formation). Third, to the west, Maastrichtian marine sediments of the Yunguilla Unit were laid down on top of the newly accreted Pallatanga Block. Taken together, these three lines of evidence suggest that the accretion of the Pallatanga Unit may well have been a protracted event that commenced in Santonian time (86–83 Ma) but was not finally completed until the end of Maastrichtian time (65 Ma). Thus the Pallatanga accretion event may have been diachronous along the length of the Cordillera.

Naranjal accretion

The accretion of the Naranjal and Macuchi Blocks onto the continental margin, the edge of which was defined by the western limit of the Pallatanga Block, took place during Eocene time. The eastern limit of both blocks is defined by the Toachi Fault and its buried southern extension, the Chimbo lineament. In the north, the continuation of the Toachi Fault is marked by the generally steeply inclined Mulaute Shear Zone (Boland *et al*.

2000; Hughes & Pilatasig 2002), where the development of a continuous belt of penetrative cleavage up to 8 km wide has been observed to the NE of San Miguel de Los Bancos (Fig. 1). Stretching lineations are often gently dipping to subhorizontal and dextral kinematic indicators, observed in several places, both within the Mulaute Shear Zone and along its continuation in the extreme south (Dunkley & Gaibor 1997) suggest an oblique emplacement from the SW for both the Naranjal and Macuchi Blocks. To the east of the Mulaute Shear Zone, ductile deformation in the north tends to be concentrated into narrower discrete cleavage zones that are separated by undeformed country rock of the Pilaton Unit. Thus the deformation associated with the accretion of the Naranjal Block can be traced over a cross-strike width of some 25 km in the northernmost segment of the Cordillera (Boland *et al*. 2000).

The timing of the Naranjal accretion is constrained by the presence of the Santiago plutons, comprising a suite of middle Eocene undeformed I-type granitoids that intrude the Naranjal Unit and yield K–Ar mineral ages ranging from 44 to 35 Ma. The undeformed nature of the Santiago plutons and occurrence of xenolithic Naranjal material within them means that the accretion of the Naranjal Block must have been complete before their emplacement (Boland *et al*. 2000). In addition, in the west the Naranjal Block is unconformably overlain by the undeformed post-accretion marine sediments of the Tortugo and Zapallo Units (Boland *et al*. 2000). Both units are rich in volcanic material and contain abundant foraminiferal remains that indicate consistent mid- to late Eocene (to possibly Oligocene) ages (see also Bristow & Hoffstetter 1977). Marine sediments of this age are common elsewhere in western Ecuador (Reynaud *et al*. 1999; Boland *et al*. 2000) and in southern Colombia (McCourt *et al*. 1990), and indicate a period of widespread marine transgression, which also heralded the beginning of a new mid-Eocene– (?)late Oligocene plutono-magmatic cycle found throughout much the Northern Andes (see also Aspden *et al*. 1987b). Detailed discussion of this event is beyond the scope of this paper, but in the northern segment of the Ecuadorian Cordillera these rocks include the Santiago plutons (Fig. 1) and mid-Eocene– (?)Oligocene volcanic-rich sediments (the Zapallo and Tortuga Units in the west and the Silante and El Laurel Units in the east) (Boland *et al*. 2000). In the south, this magmatic event is represented by the (upper) middle Eocene to Upper Miocene, intermediate to felsic, calc-alkaline volcanic rocks of the Saraguro Group (Dunkley & Gaibor 1997).

In the 0°–1°S sector of the Ecuadorian Cordillera, a single K–Ar (hornblende) age of 48 Ma has also been obtained (Hughes & Bermudez 1997) from a small syntectonic foliated diorite within the Mulaute Shear Zone. Although it is difficult to have much confidence in a single K–Ar age, when it is considered together with the evidence presented above it provides additional support for the age of the Mulaute Shear Zone and also helps to constrain the probable timing of the Naranjal accretion, which in this portion of the margin must have taken place no later than earliest mid-Eocene time.

The lower age limit for the accretion of the Naranjal Block is provided by the La Cubera Unit, which crops out to the east of the Naranjal Unit and to the west of the Mulaute Shear Zone. The unit is of Late Paleocene age and comprises cherts that pass upwards into massive sandstones. The presence of this sequence suggests that during Late Paleocene time the Naranjal Arc was still separated from the continental margin by a marine basin. However, the increasing clastic input towards the top of the unit could be interpreted to represent the initial stage of basin closure before final accretion of the Campanian Naranjal Arc.

Macuchi accretion

It has been suggested by Hughes & Pilatasig (2002) that the accretion of the more southerly Macuchi Block occurred slightly later (in Late Eocene time) than the accretion of the Naranjal Arc. In this part of the Cordillera, the Upper Paleocene to Upper Eocene Angamarca Group, which is located immediately to the east of the Macuchi Block and consists of dominantly turbiditic, quartz-rich sediments, has been interpreted as representing a basin fill sequence that was deposited between the Macuchi Arc to the west and the then continental margin (Hughes & Bermudez 1997; McCourt *et al*. 1997). The progressive closure of this basin culminated in the accretion of the Macuchi Arc during Late Eocene time, and led to both the local deformation of the older (Eocene) volcanic rocks of the Saraguro Group in the south and also to a hiatus in Saraguro volcanism (Dunkley & Gaibor 1997; Hughes & Pilatasig 2002). The presence of the undeformed Balsapamba pluton, which intruded and contact metamorphosed the Macuchi Unit to the west, has yielded concordant K–Ar biotite–hornblende mineral ages ranging from 34 to 33 Ma (McCourt *et al*. 1997). All this evidence suggests that the accretion of the Macuchi Arc was completed by Late Eocene time.

Although more precise information is required (particularly on the age of the Macuchi arc and the nature of the pre-Eocene portion of the Angamarca Group), the current evidence for the timing of accretion of the Macuchi and Naranjal Arcs appears to suggest that this event was markedly diachronous. The accretion of the Naranjal Arc appears to be reasonably well constrained and most probably occurred during early to earliest mid-Eocene time, whereas in the south the final closure of the Macuchi basin may not have taken place until Late Eocene time. A protracted Eocene accretion event may also be supported by recently published white mica and biotite $^{40}Ar/^{39}Ar$ and zircon and apatite fission-track data (Spikings *et al*. 2001) from the Cordillera Real. In addition to the Late Cretaceous cooling event already discussed, these data also contain significant evidence for a rapid (post-accretion) cooling from 43 to 30 Ma, an age span that is consistent with the deductions made here.

Accretion of the Costa units

As noted above, the timing of Macuchi volcanism is not well established, but it is probable that the cessation of activity may have been caused by the collision of the Piñon oceanic plateau with the arc before closure of the back-arc basin and the final accretion of the Macuchi Arc onto the continental margin. Although the contact between the Piñon Unit and the Macuchi is not exposed, it is probable that it is represented by a major suture, as the Macuchi and the Piñon lavas formed in such different tectonic environments. The occurrence of Late Paleocene–Early Eocene continentally derived clasts in the Azúcar sediments believed to overlie (at least in part) the Piñon Unit (Jaillard *et al*. 1995) suggests that, before its amalgamation with the Macuchi Arc, the Piñon Block was also located close to a continental margin along which no subduction was taking place. This interpretation is supported by the evidence, discussed above, for dextral fault movement in southern Ecuador during the final accretion of the Piñon–Macuchi Blocks. Furthermore, it suggests that the Piñon Block moved into its current position from a southwesterly direction, possibly along a strike-slip fault close to the continental margin before collision with the Macuchi Arc in Mid–Late Eocene time. In this context, it is also of interest to note that in spite of the fact that the Macuchi Unit and the

Angamarca Group are considered to be in part contemporaneous, the absence of proven Macuchi debris within the Angamarca sequence suggests that these units were physically separated at the time of their formation and that their present juxtaposition is the result of later tectonic transport along the Chimbo lineament.

In the 0–1°N sector of the Cordillera, the Canande Fault separates the more easterly lavas of the Naranjal Unit, which possess an island-arc signature, from those in the west, which are of oceanic plateau affinity (Fig. 1). It is therefore possible that this fault may represent the suture between the Naranjal Arc and an oceanic plateau. Thus, the cessation of magmatic activity in the Naranjal Arc in Early Maastrichtian time may have been caused by the docking of a plateau with the arc at this time. However, perhaps because the collision was oblique to the continental margin, the back-arc basin associated with the Naranjal Arc did not fully close until early to earliest mid-Eocene time.

The oceanic plateau sequences of the Costa are occasionally overlain by, and tectonically intercalated with, arc lavas. These arc lavas range in age from Cenomanian–Turonian for the Las Orquídeas Unit through Late Campanian–Maastrichtian in the Manabi area to Maastrichtian and Paleocene time in the more northerly Pedernales region (Fig. 1). The intimate tectonic association of arc and plateau lavas implies that the arc volcanism occurred, at least in part, before the Eocene collision of the Piñon and Macuchi Blocks with the continental margin. The calc-alkaline nature of this arc volcanism and its association with thickened plateau suggests that, like the Río Cala Arc that formed during accretion of the Pallatanga Unit, the San Lorenzo Arc magmas developed below, and erupted through, the thickened oceanic crust of the Piñon plateau. As the final accretion of the Piñon, Macuchi and Naranjal Blocks did not occur until Eocene time, the calc-alkaline Late Cretaceous San Lorenzo Arc must have formed in an oceanic environment.

Model of tectonic evolution

In an attempt to illustrate and help explain the observed variation in both the geology and the timing of geological events along the length of the Cordillera Occidental a series of schematic cross-sections across the Ecuadorian margin are presented in Fig. 6, and these are discussed below.

Starting in the north, we propose the following sequence of events.

(1) The Pallatanga oceanic plateau collided with the continental margin of Ecuador in Campanian time (83–74 Ma) (Fig. 6a). A subduction zone initiated at the trailing edge of the accreted plateau and gave rise to the calc-alkaline lavas of the Río Cala Arc that were erupted through the accreted Pallatanga plateau (Fig. 6b).

(2) During Late Campanian–Mid-Maastrichtian time (76–70 Ma), activity in the Río Cala Arc ceased as a new arc initiated (Naranjal) and a back-arc basin (represented by the La Portada Unit) opened between the developing Naranjal Arc and the remnants of the Río Cala Arc (Fig. 6c).

(3) Activity in the Naranjal Arc was short lived, and is believed to have been terminated by the approach and docking of an oceanic plateau in early Maastrichtian time. However, perhaps because the collision was oblique to the continental margin, the La Portada back-arc basin did not fully close until early to early mid-Eocene time (Fig. 6c).

(4) The docking of this plateau with the Naranjal plateau resulted in a back-stepping of the subduction zone to behind the trailing edge of the Piñon plateau, leading to the eruption of calc-alkaline lavas through the oceanic plateau and the formation of the San Lorenzo Arc (Fig. 6d).

(5) As a result of sustained compressive (probably dextral) stress, throughout Paleocene and early Eocene time, the La Portada back-arc basin gradually closed (Fig. 6e and f). The final closure in northern Ecuador was completed at the latest by early mid-Eocene time, and the closure is represented by the Mulaute Shear Zone.

In the more southerly parts of the Cordillera we propose that the sequence of tectonic events was as follows.

(1) Perhaps as a result of oblique collision of the plateau, the Pallatanga plateau probably commenced accretion to the southern continental margin in Late Campanian–Early Maastrichtian time (76–70 Ma), slightly later than it did in the north (Early Campanian time; 83–80 Ma) (Fig. 6a and b).

(2) Maastrichtian arc rocks, intruding or overlying the Pallatanga Unit, are absent in the southern sector of the Cordillera. However, arc rocks of this age are found in the San Lorenzo Arc, which intrudes an oceanic plateau sequence. This suggests that, following the accretion of the Pallatanga Block, subduction was initially located some distance from the continental margin (Fig. 6c).

(3) The initiation of subduction between the Piñon Plateau and the continental margin (to form the Macuchi Arc) and the cessation of activity in the southern portion of the San Lorenzo Arc, possibly in Early Paleocene time, were accompanied by the formation of a back-arc basin, in which the Angamarca sediments were deposited (Fig. 6d).

(4) The collision of the Piñon plateau with the Macuchi Arc may not have commenced until Mid-Eocene time (Fig. 6e) and resulted in the cessation of arc activity and the gradual closure of the Angamarca back-arc basin, with final accretion being completed by Late Eocene time (Fig. 6f).

Correlation with the Caribbean–Colombian Oceanic Plateau

One of the most significant aspects of this study is the recognition that the Macuchi and Naranjal island arcs separate two different oceanic plateau sequences in western Ecuador. Although these two plateaux appear to have formed at broadly the same time, their different accretion ages (Late Cretaceous and Eocene time) suggest that they did not form at the same hotspot. Although it has been maintained that the accreted Ecuadorian plateau sequences cannot be easily correlated with the Colombian sequences (Reynaud *et al*. 1999), we do not share this view. Currently available age dates of 92–84 Ma (Kerr *et al*. 1997a, 2002) place the oceanic plateau sequences in the Western and Central Cordillera of Colombia within the broad late Cretaceous time frame of the Pallatanga Unit. This, combined with the similar structural position of the Colombian and Ecuadorian (Pallatanga) terranes, makes it probable that they were originally part of the same oceanic plateau, which accreted to the Northern Andean continental margin at 85–65 Ma. A significant proportion of the oceanic plateau now preserved in and around the Caribbean basin is of the same age (93–85 Ma; Sinton *et al*. 1998), and this material appears to have begun to move into the Proto-Caribbean seaway from the Pacific from about 85 Ma onwards (e.g. White *et al*. 1999). Taken together, these lines of evidence from the Caribbean and its margins suggest that the accreted Late Cretaceous oceanic plateau sequences in the Cordillera of the Northern Andes may well belong to the same oceanic plateau, the Caribbean–Colombian Oceanic Plateau (CCOP).

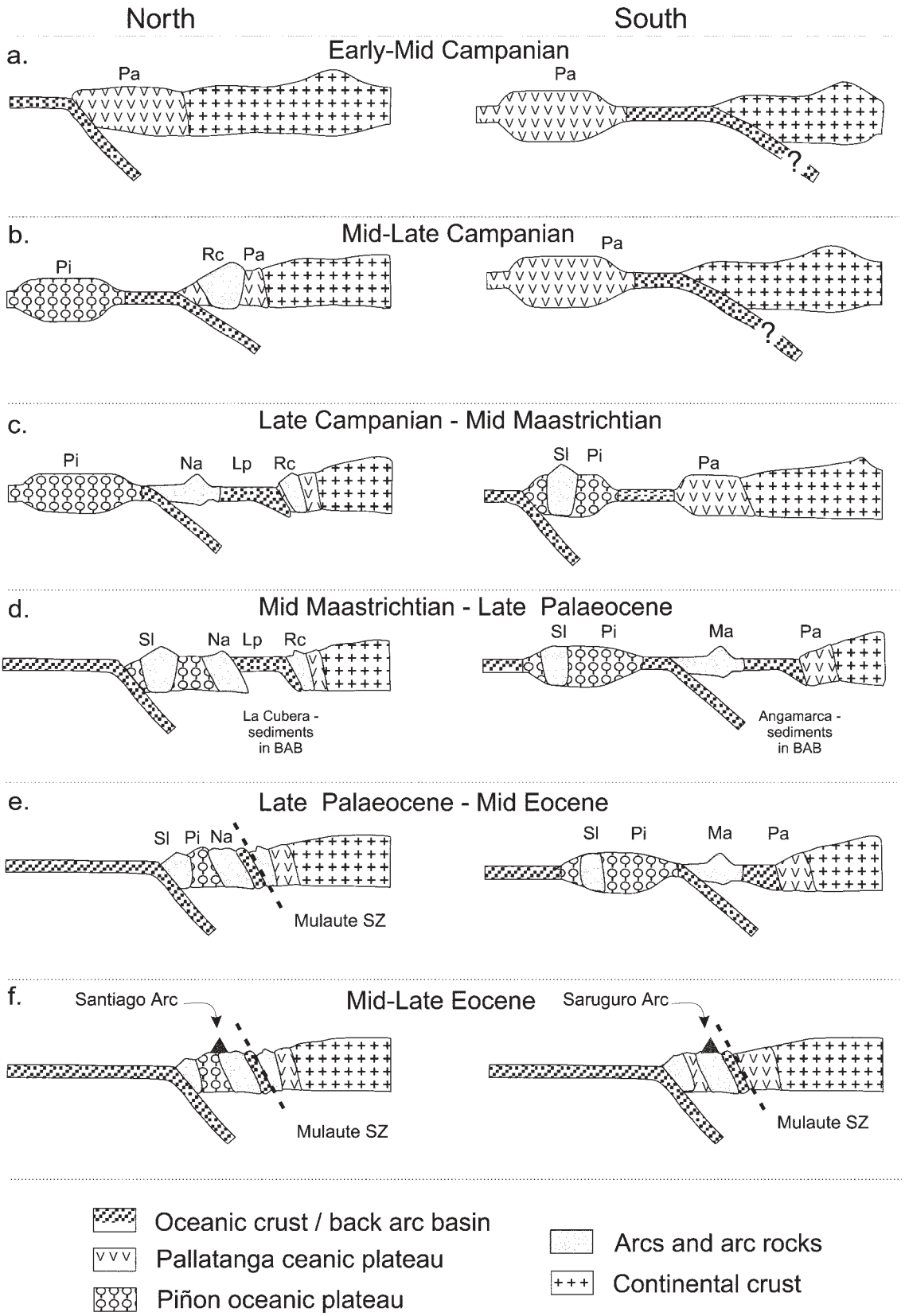

Fig. 6. Schematic cross-sections (all from west to east) depicting the tectonic development of the Ecuadorian continental margin in the north (0°) and in the south (2°S). (See text for full discussion of this model.) Pa, Pallatanga; Rc, Río Cala; Lp, La Portada; Sl, San Lorenzo; Pi, Piñon; Ma, Macuchi; Na, Naranjal. BAB, back-arc basin; SZ, shear zone.

However, the evidence from this study sheds new light on the interpretation of the accreted oceanic plateaux preserved in the coastal regions of Colombia and Ecuador. The oceanic plateau sequences in question are those of the Piñon and Esmeraldas–Pedernales regions combined with the basalts of the SerranÍa de Baudó in Northern Colombia (Kerr *et al*. 1997a), and the komatiites, picrites and basalts of Gorgona Island, 50 km west of the Colombian coast at *c*. 3°N (Kerr *et al*. 1996). We contend that these sequences are not part of the CCOP, *sensu stricto*, as they are in large part separated from the Cordilleran oceanic sequences by Late Cretaceous–Early Tertiary island-arc terranes. Additionally, these sequences are characterized by generally more depleted trace element and radiogenic isotopic signatures than those of the Cordillera and the Caribbean (Kerr *et al*. 1997a, 1997b). Further support for the proposal of a different plateau is provided by new Hf isotope ratios from the komatiites of Gorgona Island (Thompson 2002), which are markedly different from those of the CCOP. Given the potentially older age of the Piñon Unit, combined with the likelihood that it was accreted from a more southerly direction and the fact that it is separated from the Esmeraldas–Pedernales sequences by the Puerto Cayo–Canande Fault Zone, it is possible that Piñon represents a different plateau from the Esmeraldas–Pedernales, SerranÍa de Baudó and Gorgona sequences.

A corollary of the evidence for two separate oceanic plateau events with similar igneous emplacement ages but different tectonic accretion ages, is that these two plateaux cannot have formed from the same mantle plume or hotspot. It has been long been proposed that the CCOP formed at the start-up phase of the Galápagos hotspot (Richards *et al*. 1991; Storey *et al*. 1991); however, it has been suggested by Revillon *et al*. (2000) that at least some of the Caribbean and Northern Andean Cretaceous oceanic plateau sequences have been derived from the Sala y Gomez hotspot (currently located 3000 km SW of the Caribbean at 33°S, 110°W). In addition, palaeomagnetic evidence from Gorgona Island (Estrada & MacDonald 1994) has suggested that the lavas cannot have formed at the Galápagos hotspot, but rather originate from a much more southerly latitude.

Conclusions

(1) A wide variety of accreted oceanic igneous terranes of Late Cretaceous to Early Tertiary age are preserved in Western Ecuador; these include oceanic plateau material, calc-alkaline arc rocks erupted through thickened oceanic plateau, island-arc sequences and their associated back-arc basins.

(2) Two main accretionary phases can be recognized in western Ecuador. The first appears to have been a relatively prolonged (10–20 Ma), Late Cretaceous event and corresponds to the accretion of the Pallatanga (oceanic plateau) Unit. The second accretion event spans early to late Eocene time and marks the accretion of the Naranjal and Macuchi Units (island arcs) along with the Piñon and Pedernales–Esmeraldas oceanic plateau sequences.

(3) The oceanic plateau sequences of the Cordilleran Pallatanga and the coastal Piñon–Pedernales–Esmeraldas are separated by the Late Cretaceous to Early Tertiary Naranjal and Macuchi island arcs.

(4) As the two plateau sequences of very similar ages are separated by accreted island arcs they cannot be part of the same oceanic plateau or have formed at the same hotspot. The Pallatanga Unit can be correlated with, and probably belongs to, the same oceanic plateau as those sequences exposed both in the Western and possibly the Central Cordillera of Colombia and within and around the Caribbean region. The Piñon–Pedernales–Esmeraldas Units represent a part of one (and possibly two) different oceanic plateau(x) which are also preserved on Gorgona Island and the Serranía de Baudó in Colombia. These plateau sequences may have been generated by the Sala y Gomez plume.

We acknowledge invaluable discussions on Caribbean and North Andean geology with our colleagues: A. Saunders, R. White, M. Weber, P. Thompson, A. Nivia, F. Alcocer, A. Eguez and E. Jaillard; we thank them all. In addition, J.A.A. would like to thank all the members of BGS–CODIGEM team; many of the findings presented here (although not necessarily the interpretations) are a direct result of their efforts. In particular, J.A.A. thanks W. McCourt for his support and over the years the many discussions relating to the evolution of the Northern Andes. The work of the BGS in Ecuador was partly funded by the British Government via the Department for International Development, and was carried out as part of the World Bank sponsored Mining Development and Environmental Control Technical Assistance Project. J.A.A. publishes with the permission of the Director of the British Geological Survey. I. MacDonald provided assistance with ICP-MS analyses at Cardiff, and N. Marsh with XRF facilities at Leicester. Constructive reviews by M. Tejeda, R. Arculus and C. Neal are appreciated.

References

Abbott, D. & Mooney, W. 1995. The structural and geochemical evolution of the continental crust: support for the oceanic plateau model of continental growth. *Reviews of Geophysics*, **33**, 231–242.

Aspden, J.A. & Litherland, M. 1992. The geology and Mesozoic collisional history of the Cordillera Real, Ecuador. *Tectonophysics*, **205**, 187–204.

Aspden, J.A., Fortey, N., Litherland, M., Viteri, F. & Harrison, S.M. 1992*a*. Regional S-type granites in the Ecuadorian Andes—possible remnants of the breakup of Western Gondwana. *Journal of South American Earth Sciences*, **6**, 123–132.

Aspden, J.A., Harrison, S.H. & Rundle, C.C. 1992*b*. New geochronological control for the tectonomagmatic evolution of the metamorphic basement, Cordillera Real and El-Oro Province of Ecuador. *Journal of South American Earth Sciences*, **6**, 77–96.

Aspden, J.A., Litherland, M., Duque, P., Salazar, E., Bermudez, R. & Viteri, F. 1987*a*. Nuevo cinturon ofiolítico en la Cordillera Real, Ecuador y su posible significacion regional. *Politecnica, Monografia de Geologia*, **5**(XII(2)), 80–93.

Aspden, J.A., McCourt, W.J. & Brook, M. 1987*b*. Geometrical control of subduction-related magmatism: the Mesozoic and Cenozoic plutonic history of western Colombia. *Journal of the Geological Society, London*, **144**, 893–905.

Boland, M.L., Pilatasig, L.F., Ibadango, C.E., McCourt, W.J., Aspden, J.A., Hughes, R.A. & Beate, B. 2000. *Geology of the Cordillera Occidental of Ecuador between 0° and 1°N*. Proyecto de Desarrollo Minero y Control Ambiental, Programa de Informacion Cartografica y Geologica, CODIGEM–BGS, Quito, Informe **10**.

Bristow, C.R. & Hoffstetter, R. 1977. *Lexique Stratigraphique International; Ecuador*, *2nd*. Centre National de la Recherche Scientifique, Paris.

Condie, K.C. & Abbott, D.H. 1999. Oceanic plateaus and hotspot islands: identification and role in continental growth. *Lithos*, **46**, 1–4.

Cosma, L., Lapierre, H., Jaillard, E. & 5 others 1998. Petrography and geochemistry of the magmatic units of the Western Cordillera of Ecuador (0°30′S); tectonic implications. *Bulletin de la Société Géologique de France*, **169**, 739–751.

Dunkley, P. & Gaibor, A. 1997. *Geology of the Cordillera Occidental of Ecuador between 2–3°S*. Proyecto de Desarollo Minero y Control Ambiental, Programa de Informacion Cartografica y Geologica, CODIGEM–BGS, Quito, Informe **2**.

Eguez, A. 1986. *Evolution Cénozoíque de la Cordillére Occidentale Septenrionale d'Equateur (0°15′S–1°10′S). Les minéralisation associées*. PhD thesis, Université Pierre et Marie Curie, Paris.

Eguez, A. & Aspden, J.A. 1993. The Mesozoic–Cenozoic evolution of the Ecuadorian Andes. *Andean Geodynamics, Extended Abstracts*. ORSTOM/Oxford University, Paris/Oxford, 179–182.

Estrada, J.J. & MacDonald, W.D. 1994. Andean accretionary Cretaceous terranes; paleomagnetic evidence supporting large latitudinal displacement component at Gorgona Island, Colombia. *EOS Transactions, American Geophysical Union*, **75**, 127.

Faucher, B. & Savoyat, E. 1973. Esquisse géologique des Andes de l'Equateur. *Revue de Géographie Physique et de Géologie Dynamique*, **15**, 115–142.

Goosens, P.J. & Rose, W.I. 1973. Chemical composition and age determination of tholeiitic rocks in the Basic Igneous Complex, Ecuador. *Geological Society of America Bulletin*, **84**, 1043–1052.

Henderson, W.G. 1979. Cretaceous to Eocene volcanic arc activity in the Andes of northern Ecuador. *Journal of the Geological Society, London*, **136**, 367–378.

Hughes, R.A. & Bermudez, R. 1997. *Geology of the Cordillera Occidental of Ecuador between 0–1°S*. Proyecto de Desarollo Minero y Control Ambiental, Programa de Informacion Cartografica y Geologica, CODIGEM–BGS, Quito, Informe **4**.

Hughes, R.A. & Pilatasig, L.F. 2002. Cretaceous and Tertiary terrane accretion in the Cordillera Occidental of the Andes of Ecuador. *Tectonophysics*, **345**, 29–48.

Jaillard, E., Ordonez, M., Benitez, S., Berrones, G., Jimenez, N., Montenegro, G. & Zambrano, I. 1995. Basin development in an accretionary, oceanic-floored fore-arc setting: southern coastal Ecuador during late Cretaceous time. *In:* Tankard, A.J., Suarez, S. & Welsink, H.J. *Petroleum Basins of South America*. AAPG Memoir, **62**, 615–631.

Jolly, W.T., Lidiak, E.G., Dickin, A.P. & Wu, T.W. 2001. Secular geochemistry of central Puerto Rican island arc lavas: constraints on Mesozoic tectonism in the eastern Greater Antilles. *Journal of Petrology*, **42**, 2197–2214.

Kerr, A.C. 1998. Oceanic plateau formation: a cause of mass extinction and black shale deposition around the Cenomanian–Turonian boundary. *Journal of the Geological Society, London*, **155**, 619–626.

Kerr, A.C. & Arndt, N.T. 2001. A note on the IUGS reclassification of the high-Mg and picritic volcanic rocks. *Journal of Petrology*, **42**, 2169–2171.

Kerr, A.C., Marriner, G.F., Arndt, N.T., Tarney, J., Nivia, A., Saunders, A.D. & Duncan, R.A. 1996. The petrogenesis of komatiites, picrites and basalts from the Isle of Gorgona, Colombia; new field, petrographic and geochemical constraints. *Lithos*, **37**, 245–260.

Kerr, A.C., Marriner, G.F., Tarney, J., Nivia, A., Saunders, A.D., Thirlwall, M.F. & Sinton, C.W. 1997a. Cretaceous basaltic terranes in western Colombia: elemental, chronological and Sr–Nd constraints on petrogenesis. *Journal of Petrology*, **38**, 677–702.

Kerr, A.C., Tarney, J., Kempton, P.D., Spadea, P., Nivia, A., Marriner, G.F. & Duncan, R.A. 2002. Pervasive mantle plume head heterogeneity: evidence from the late Cretaceous Caribbean–Colombian Oceanic Plateau. *Journal of Geophysical Research*, in press.

Kerr, A.C., Tarney, J., Marriner, G.F., Nivia, A. & Saunders, A.D. 1997b. The Caribbean–Colombian Cretaceous igneous province: the internal anatomy of an oceanic plateau. *In:* Mahoney, J.J. & Coffin, M. *Large Igneous Provinces; Continental, Oceanic and Planetary Flood Volcanism*. Geophysical Monograph, American Geophysical Union, **100**, 45–93.

Kerrich, R., Wyman, D., Hollings, P. & Polat, A. 1999. Variability of Nb/U and Th/La in 3.0 to 2.7 Ga Superior Province ocean plateau basalts: implications for the timing of continental growth and lithosphere recycling. *Earth and Planetary Science Letters*, **168**, 101–115.

Lapierre, H., Bosch, D., Dupuis, V. & 12 others 2000. Multiple plume events in the genesis of the peri-Caribbean Cretaceous oceanic plateau province. *Journal of Geophysical Research*, **105**, 8403–8421.

Lebrat, M., Megard, F., Dupuy, C. & Dostal, J. 1987. Geochemistry and tectonic setting of pre-collision Cretaceous and Paleogene volcanic rocks of Ecuador. *Geological Society of America Bulletin*, **99**, 569–578.

Lebrat, M., Megard, F., Juteau, T. & Calle, J. 1985. Pre-orogenic assemblages and structure in the Western Cordillera of Ecuador. *Geologische Rundschau*, **74**, 343–351.

Litherland, M. & Aspden, J.A. 1992. Terrane boundary reactivation—a control on the evolution of the Northern Andes. *Journal of South American Earth Sciences*, **5**, 71–76.

Litherland, M., Aspden, J.A. & Jemielita, R.A. 1994. *The Metamorphic Belts of Ecuador*. British Geological Survey, Overseas Memoir, **11**.

McCourt, W.J., Aspden, J.A. & Brook, M. 1984. New geological and geochronological data from the Colombian Andes: continental growth by multiple accretion. *Journal of the Geological Society, London*, **141**, 831–845.

McCourt, W.J., Duque, P. & Pilatasig, L.F. 1997. *Geology of the Western Cordillera of Ecuador between 1–2°S*. Proyecto de Desarrollo Minero y Control Ambiental, Programa de Informacion Cartografica y Geologica, CODIGEM–BGS, Quito, Informe **3**.

McCourt, W.J., Muñoz, U. & Villegas, V. 1990. *Regional geology and gold potential of the Guapi–Napi drainage basin and upper Timbiqui river, Cauca Department, SW Colombia*. British Geological Survey, Overseas Geology Series, Technical Report WC/90/34.

Millward, D., Marriner, G.F. & Saunders, A.D. 1984. Cretaceous tholeiitic volcanic rocks from the Western Cordillera of Colombia. *Journal of the Geological Society, London*, **141**, 847–860.

Nielsen, R.L. 1988. A model for the simulation of combined major and trace element liquid lines of descent. *Geochimica et Cosmochimica Acta*, **52**, 27–38.

Polat, A., Kerrich, R. & Wyman, D.A. 1998. The late Archean Schreiber–Hemlo and White River Dayohessarah greenstone belts, Superior Province: collages of oceanic plateaus, oceanic arcs, and subduction–accretion complexes. *Tectonophysics*, **289**, 295–326.

Pratt, W.T., Figueroa, J. & Flores, B. 1997. *Geology of the Cordillera Occidental of Ecuador between 3–4°S*. Proyecto de Desarollo Minero y Control Ambiental, Programa de Informacion Cartografica y Geologica, CODIGEM–BGS, Quito, Informe **1**.

Puchtel, I.S., Hofmann, A.W., Mezger, K., Jochum, K.P., Shchipansky, A.A. & Samsonov, A.V. 1998. Oceanic plateau model for continental crustal growth in the Archaean, a case study from the Kostomuksha greenstone belt, NW Baltic Shield. *Earth and Planetary Science Letters*, **155**, 57–74.

Revillon, S., Hallot, E., Arndt, N.T., Chauvel, C. & Duncan, R.A. 2000. A complex history for the Caribbean plateau: petrology, geochemistry, and geochronology of the Beata Ridge, south Hispaniola. *Journal of Geology*, **108**, 641–661.

Reynaud, C., Jaillard, E., Lapierre, H., Mamberti, M. & Mascle, G.H. 1999. Oceanic plateau and island arcs of southwestern Ecuador; their place in the geodynamic evolution of northwestern South America. *Tectonophysics*, **307**, 235–254.

Richards, M.A., Jones, D.L., Duncan, R.A. & DePaolo, D.J. 1991. A mantle plume initiation model for the formation of Wrangellia and other oceanic flood basalt plateaus. *Science*, **254**, 263–267.

Sauer, W. 1965. *Geologia del Ecuador*. Ministerio de Educacion Publica, Quito.

Sinton, C.W., Duncan, R.A., Storey, M., Lewis, J. & Estrada, J.J. 1998. An oceanic flood basalt province within the Caribbean plate. *Earth and Planetary Science Letters*, **155**, 221–235.

Spadea, P. & Espinosa, A. 1996. Petrology and chemistry of late Cretaceous volcanic rocks from the southernmost segment of the Western Cordillera of Colombia (South America). *Journal of South American Earth Sciences*, **9**, 79–90.

Spikings, R.A., Winkler, W., Seward, D. & Handler, R. 2001. Along-strike variations in the thermal and tectonic response of the continental Ecuadorian Andes to the collision with heterogeneous oceanic crust. *Earth and Planetary Science Letters*, **186**, 57–73.

Stein, M. & Goldstein, S.L. 1996. From plume head to continental lithosphere in the Arabian–Nubian shield. *Nature*, **382**, 773–778.

Storey, M., Mahoney, J.J., Kroenke, L.W. & Saunders, A.D. 1991. Are oceanic plateaus sites of komatiite formation? *Geology*, **19**, 376–379.

Sun, S.-s. & McDonough, W.F. 1989. Chemical and isotope systematics of oceanic basalts: implications for mantle composition and processes. *In:* Saunders, A.D. & Norry, M.J. *Magmatism in the Ocean Basins*. Geological Society, London, Special Publications, **42**, 313–345.

Tschopp, H.J. 1948. Geological sketch of Ecuador. *Bulletin de l'Association Suisse de Géologie Ingénieur et Pétrologie*, **15**, 14–45.

Thompson, P.M.E. 2002. *Petrology and geochronology of an arc sequence, Bonaire, Dutch Antilles, and its relationship to the Caribbean Plateau*. PhD thesis, University of Leicester.

Van Thournout, F. 1991. *Stratigraphy, magmatism and tectonism in the Ecuadorian Northwest Cordillera: metallogenic and geodynamic implications*. PhD thesis, Katholieke Universiteit, Leuven.

Van Thournout, F., Hertogen, J. & Quevedo, L. 1992. Allochthonous terranes in northwestern Ecuador. *Tectonophysics*, **205**, 205–221.

White, R.V., Tarney, J., Kerr, A.C., Saunders, A.D., Kempton, P.D., Pringle, M.S. & Klaver, G.T. 1999. Modification of an oceanic plateau, Aruba, Dutch Caribbean: implications for the generation of continental crust. *Lithos*, **46**, 43–68.

Wolf, T. 1892. *Geografia y Geologia del Ecuador*. Brockhaus, Leipzig.

Received 8 November 2001; revised typescript accepted 28 March 2002.
Scientific editing by Sally Gibson